Integrating Environmental Variables with WorldView-2 Data to Model the Probability of Occurrence of Invasive *Chromolaena odorata* in Forest Canopy Gaps: Dukuduku Forest in KwaZulu-Natal, South Africa

By

OUPA MALAHLELA

212560886

Supervisor: Prof. Onisimo Mutanga

Co-supervisor: Dr. Moses Cho

Submitted in fulfilment of the academic requirements for the degree Master of Science in the School of Agriculture, Earth and Environmental Sciences in the College of Agriculture, Engineering and Science. University of KwaZulu-Natal, Pietermaritzburg

October 2013

DECLARATION 1

This study was undertaken in fulfilment of a Master's Degree and presents the original work of the author. Any work taken from other authors or organizations is duly acknowledged within the text and references section.

.....

Mr. Oupa Malahlela
(Student)

.....

Prof. Onisimo Mutanga
(Supervisor)

.....
Dr. Moses Cho
(Supervisor)

DECLARATION 2

DETAILS OF CONTRIBUTION TO PUBLICATIONS that form part of and/or include research presented in this thesis (includes publications in preparation, submitted, in press and published and give details of the contributions of each author to the experimental work and writing of each publication).

> **Publication 1**: Malahlela, O.E [1, 2], Mutanga, O [1]. Cho, M.A [1, 2]. (in press). Mapping canopy gaps in an indigenous subtropical coastal forest using high resolution Worldview-2 image.

The work was done by the first author under the guidance and supervision of second and third authors.

> **Publication 2**: Malahlela, O.E [1, 2]. Cho, M.A [1,2]., Mutanga, O [1]. (in preparation). Integrating environmental and WorldView-2 data to map the probability of occurrence of invasive *Chromolaena odorata* in forest gaps, Dukuduku coastal forest in South Africa.

The work was done by the first author under the guidance and supervision of second and third authors.

[1] University of KwaZulu-Natal, Discipline of Geography, P. Bag X01, Scottsville, 3209, Pietermaritzburg, South Africa.

[2] Council for Scientific and Industrial Research (CSIR), Natural Resources and Environment, Earth Observation Unit, P. O. Box 395, Pretoria, 0001, South Africa.

Signed: .....

Table of Contents

List of Figures

List of Tables

Acronyms

ARVI – Atmospherically resistant vegetation index

ATCOR – Atmospheric / Topographic Correction for Satellite Imagery

AUC – Area under curve

D^2 – Deviance

DEM – Digital Elevation Model

ESRI – Environmental Science Research Institute

EVI – Enhanced vegetation index

FSTEDGE – Forest edges

GAPPRMT – Gap perimeter (in square meters)

GAPSIZE – Forest gap size (in square meters)

GPS – Global Positioning System

Landsat TM – Landsat Thematic Mapper

LiDAR – Light Detection and Ranging

MDC – Minimum distance classifier

MLC – Maximum likelihood classifier

MODTRAN – MODerate resolution atmospheric TRANsmission

mPSRI – Modified plant senescence reflectance index

NDVI – Normalized difference vegetation index

$NDVI_{545}$ – Green normalized difference vegetation index

$NDVI_{605}$ – Yellow normalized difference vegetation index

$NDVI_{660}$ – Red normalized difference vegetation index

$NDVI_{725}$ – Red edge normalized difference vegetation index

$NDVI_{830}$ – Near infrared normalized difference vegetation index

NIR – Near infrared band

NPCI – Normalized pigment chlorophyll index

OBIA – Object-based image analysis

PBIC – Pixel based image classification

PPC – Parallelepiped classifier

RDDIST – Distance to roads/paths

RGB – Red, Green, Blue bands

ROC – Receiver operating characteristic

RVDIST – Distance to the rivers/streams

SAVI – Soil-adjusted vegetation index

SPOT – Système Pour l'Observation de la Terre

WV-2 – WorldView-2

YI – Yellowness index

Abstract

Several alien plants are invading subtropical forest ecosystems through canopy gaps, resulting in the loss of native species biodiversity. The loss of native species in such habitats may result in reduced ecosystem functioning. The control and eradication of these invaders requires accurate mapping of the levels of invasion in canopy gaps. Our study tested (i) the utility of WorldView-2 imagery to map forest canopy gaps, and (ii) an integration of WorldView-2 data with environmental data to model the probability of occurrence of invasive *Chromolaena odorata* (triffid weed) in Dukuduku forest canopy gaps of KwaZulu-Natal, South Africa. Both pixel-based classification and object-based classification were explored for the delineation of forest canopy gaps. The overall classification accuracies increased by ± 12% from a spectrally resampled 4 band image similar to Landsat (74.64%) to an 8 band WorldView-2 imagery (86.90%). This indicates that the new bands of WorldView such as the red edge band can improve on the capability of common red, blue, green and near-infrared bands in delineating forest canopy gaps. The maximum likelihood classifier (MLC) in pixel-based classification yielded the overall classification accuracy of 86.90% on an 8 band WorldView-2 image, while the modified plant senescence reflectance index (mPSRI) in object-based classification yielded 93.69%. The McNemar's test indicated that there was a statistical difference between the MLC and the mPSRI. The mPSRI is a vegetation index that incorporates the use of the red edge band, which solves a saturation problem common in sensors such as Landsat and SPOT.

An integrated model (with both WorldView-2 data and environmental data) used to predict the occurrence of *Chromolaena odorata* in forest gaps yielded a deviance of about 42% (D^2 = 0.42), compared to the model derived from environmental data only (D^2 = 0.12) and WorldView-2 data only (D^2 = 0.20). A D^2 of 0.42 means that a model can explain about 42% of the variability of the presence/absence of *Chromolaena odorata* in forest gaps. The Distance to Stream and Aspect were the significant environmental variables ($\rho < 0.05$) which were positively correlated with presence/absence of *Chromolaena* in forest gaps. WorldView-2 bands such as the coastal band (λ_{425} nm) yellow band (λ_{605} nm) and the near-infrared-1 (λ_{833} nm) are positively and significantly related to the presence/absence of invasive species ($\rho < 0.05$). On the other hand, a significant negative correlation ($\rho < 0.05$) of near-infrared-2 band (λ_{950} nm) and the red edge normalized difference vegetation index ($NDVI_{725}$) suggests that the probability of occurrence of invasive *Chromolaena* increases in

forest gaps with low vegetation density. This study highlights the importance of WorldView-2 imagery and its application in subtropical indigenous coastal forest monitoring.

Acknowledgements

I would like to express my earnest gratitude to the following people and the institutions for their contribution to this research:

- Dr. Moses Cho from the CSIR, who helped me continuously from the planning, analysis, and final write-up of this research. A special "thank-you" for his personal advices and mentoring skills exhibited throughout my postgraduate study.

- I would like to extend my gratitude to Prof. Onisimo Mutanga from Discipline of Geography at UKZN, for guiding me towards the completion of this research. His academic merit was of great importance to the production of this document.

- I would like to thank Ms. Nontembeko Dudeni-Tlhone for her significant statistical contribution and her support whenever I needed her. I also thank Dr. Pravesh Debba for his allowing me to use their facilities and their expertise.

- I would like to thank Prof. Chris Munyati for the undivided encouragement to develop science attitude and to inspire my persistence in the field of remote sensing.

- I wish to thank Laven Naidoo for proof-reading the document and for correcting grammatical errors.

- I thank Earth Observation colleagues Abel, Sabelo, Heidi, Nobuhle, Russell and Renaud for their contribution to my work.

- I would like to thank my family and friends for their understanding and support towards my studies. To Ethel Seabela, my ex-companion and my son Tino.

- I thank the Mandela-Rhodes Foundation for making a significant contribution to lay the foundation of my postgraduate studies. Special thanks to the late Prof. Jake Gerwel for his motivation to do the best for our continent.

- I extend my appreciation also to the Department of Science and Technology for financial support. They made this project possible.

- I would like to thank the Department of Forestry and Fisheries for permitting me to conduct a research at their protected area.

- Thank you to S'bu Gumede of Khula village in KwaZulu-Natal for assisting in data collection.

- I thank Dr. George Tengbeh, Mr. Reuben Ramudzuli, Dr. Brilliant Petja, Ms. Josephine Letsoalo at the Department of Geography at the University of Limpopo for their guidance in my undergraduate studies.
- I would like to extend my appreciation to Mr. Joe Moila, Mr. Matome B. Malatjie, Seleka Makhura, Ms Phuti M. Mokobodi, Mr. Cisco M. Moila, Mr. Martin Mundluli, Mr. Teenage F. Malegopo, Mr. Nakampe P Lebepe and Mr. Thivhileli A. Ratshivhadelo for being the source of motivation and encouragement at my primary and high school levels.
- Special thanks to my sisters Ceciliah, Kabelo and Nthuse for their unconditional love and support. I would like to express my sincere gratitude to Walter Mohale and Carlton Mamorobela, my childhood friends, for being so supportive and tolerant with me throughout my secondary and tertiary studies.
- To Tshepiso and Tino.

Chapter One

Introduction

1.1 Study background

Subtropical forests form a crucial part of global ecosystems and provide habitat to a variety of biodiversity (Anon, 1997). However, their importance has been threatened by human-induced activities such as natural forest-logging, agricultural practices, land degradation, settlement expansion and as well as the occurrence of invasive species in the intact forests (Felton et al., 2006; Merriam, 1988; Zedler and Scheid, 1988). Recently, the indigenous forest threat posed by invasive species has received increased attention from the researchers and forest managers globally (Holm et al., 1977; Lamb, 1988; Joshi et al, 2006). Invasive plant species are non-native species that alter ecosystem structure and function of an indigenous plant community (Weiss and Noble, 1984). In the subtropical forests of South Africa, *Chromolaena odorata* is known to be a common invasive species.

The invasive *Chromolaena odorata* was firstly introduced as a garden plant in KwaZulu-Natal, South Africa, around 1947 and became invasive around 1960 (Oosthuizen, 1964). Invasive *Chromolaena* is a perennial shrubby species (family = *Asteraceae*) that forms dense thickets of about 2.5 meter tall (Luwum, 2002). It has reached alarming proportions in South Africa and extended to some parts of Swaziland (Goodall and Erasmus, 1996). Currently, this invasive species is well-established in South Africa and it is classified as one of the most harmful species on the list of invaders (Boon, 2010). In the indigenous forest ecosystem, this species often takes advantage of the forest gaps for growth and reproduction, and its seed propagation rate worsen the invasion (Totland et al., 2005). It, therefore, becomes imperative to identify these forest gaps as they form crucial habitats for invasive species occurrence in the tropical forests.

Previous studies have been undertaken to identify the forest canopy gaps. The identification of forest canopy gaps was done using common methods, which included intensive manual delineation and visual interpretation of aerial photographs (Battles et al., 1996; Brokaw and Grear, 1991). Although these methods proved successful in several instances, the challenge rests in their implementation on larger and wider landscapes. To overcome this problem, remote sensing technology is increasingly being utilised in studying forest gaps in larger areas, and those that are physically inaccessible. For example Negrón-Juárez (2011) used

Landsat imagery to delineate forest gaps in the Brazilian Amazon. However, the difficulty of applying coarse resolution imagery such as Landsat (> 30 m spatial resolution) is apparent in areas where forest gaps are less than the size of the pixel. On the other hand, saturation of reflectance in the visible-near infrared region in a closed canopy environment, poses a serious challenge when using these sensors (Knipling, 1970). To mitigate the saturation problem, the use of hyperspectral data is suggested as an effective means to study invasive species and forest gaps more accurately (Betts et al., 2005; Lefsky et al., 2002; Andrew and Ustin, 2008). This technology has not been fully explored due to the high cost associated with the acquisition of these datasets (Wolter et al., 2009). The availability of commercial multispectral sensors with high spatial and spectral resolution provides opportunities for improved study of vegetation characteristics (Mutanga et al., 2012, Cho et al., 2012).

One such multispectral sensor is WorldView-2 with 8 multispectral bands and a 2 meter spatial resolution. To the best of our knowledge, the sensor has not been tested to study forest gaps and invasive species in a tropical environment. WorldView-2 has four new spectral bands (coastal, red-edge, yellow and NIR2) in addition to what the common sensors such as Landsat TM and SPOT have, which could allow an in-depth study of invasive species and forest gaps (Digital Globe, 2009). These bands are strategically positioned at wavelengths that maximize sensitivity to changes in vegetation status, such as greenness and biomass (Mutanga and Skidmore, 2004; Omar, 2010). WorldView-2 sensor consists of a red edge band (725 nm), among other bands, that has improved the estimation of forest biophysical characteristics (Mutanga et al., 2012). These findings served as a basis for testing an assumption that WorldView-2 can be used to delineate forest canopy gaps and assessing the probability of occurrence of *Chromolaena odorata* in such gaps.

Several approaches have been suggested in order to delineate forest canopy gaps. For example, Fox et al. (2000) used a combination of manual digitization and aerial photography to extract forest canopy gaps. On the other hand, Negrón-Juárez et al. (2011) used spectral mixture analysis on Landsat image to map the occurrence of forest gaps in central Amazon. Most of the studies that have successfully delineated forest gaps have relied on common pixel-based classifiers such as maximum-likelihood, minimum distance, parallelepiped and spectral angle mapper classifiers (Mallinis et al., 2008; Kim et al., 2009). However, forest gaps are not spatially similar throughout the entire forest. They have different lengths, sizes, depth and texture characteristics, and pixel-based classification does not address these attributes. Therefore, accurate classification of such gaps may require techniques that can

take into account variation in gap characteristics – not merely their spectral property. In the light of this background, this study explores the utility of new generation WorldView-2 satellite imagery and object-based approaches to map the presence/absence of *Chromolaena odorata* in forest canopy gaps in the Dukuduku coastal forest of KwaZulu-Natal, South Africa. To achieve this main aim, the study sets itself the following objectives:

1. Explore the utility of WorldView-2 multispectral bands for delineating forest canopy gaps
2. Investigate the performance of object-based classification technique over pixel-based classification methods for delineating forest canopy gaps.
3. Investigate whether integration of remote sensing and ancillary data can improve the prediction of *Chromolaena odorata* presence/absence in forest gaps

1.2 Outline of Thesis

This thesis consists of four (4) chapters. Chapter 1 presents the background of the study, aims and objectives of the study. Chapter 2 and 3 were written in the form of papers for submission to peer reviewed journals. Chapter 2 presents the delineation of invasive species habitats, i.e. forest gaps, in the subtropical coastal forest of KwaZulu-Natal. Highlights on data and delineation techniques are discussed in full in this chapter. Chapter 3 presents mapping of invasive *Chromolaena odorata* in forest gaps using logistic regression models, geographic information systems (GIS) and WorldView-2 remote sensing data. Chapter 4 presents conclusion of the study, highlighting important findings of the study. The aims and the objectives of the study are highlighted in this chapter. At the end of this chapter, the limitations of the study and recommendations for future investigations are outlined.

1.3 General methodology

This study first explored the utility of WorldView-2 data to delineate forest canopy gaps in Dukuduku coastal forest, by employing pixel-based classification and object-based classification with vegetation indices as proxies. The delineated maps were then used to generate forest gap parameters such as size that were, in turn, used as supplementary environmental data for mapping the probability of occurrence of *Chromolaena odorata* in

forest canopy gaps. The second part of the study involved integrating ancillary data with WorldView-2 bands in a stepwise logistic regression to model the probability of occurrence of invasive *Chromolaena odorata* in forest gaps (fig.1).

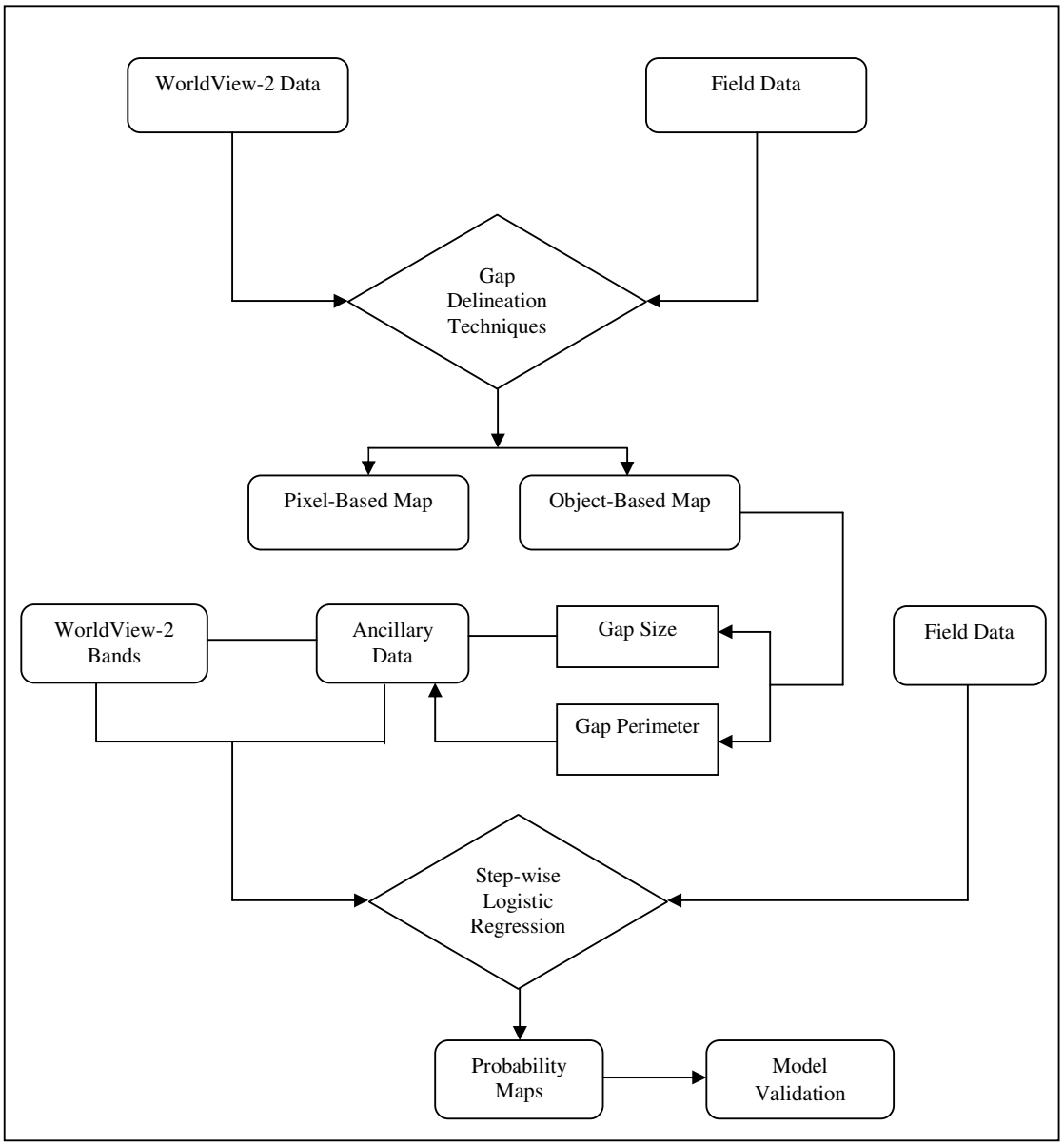

Fig. 1 A diagram that shows the general methodology of the research. WorldView-2 data was used to derive forest gap characteristics (type, size and perimeter) which were later used in combination with supplementary environmental data and WV-2 bands to map the probability of occurrence of *Chromolaena odorata* in forest gaps.

Chapter Two

Mapping Canopy Gaps in an Indigenous Coastal Forest of Dukuduku in KwaZulu-Natal, Using Worldview-2 Imagery[1]

2.1 Abstract

Canopy gaps play an important ecological role in tropical and subtropical forests. They are known to be created by tree-falls, timber harvesting or any other catastrophic disturbances. Naturally, indigenous tree regeneration in forest canopy gaps closes up the gaps and thereby increases native tree species biomass. However, invasive species may take advantage of such gaps and eventually colonize them, which may result in the loss of native species recruitment. Therefore, an understanding of the location and distribution of canopy gaps will assist in predicting the occurrence of invasive species in such canopy gaps. In this study, we tested the utility of WorldView-2 with eight (8) spectral bands at a 2 meter spatial resolution to delineate forest gaps in Dukuduku Coastal Forest, South Africa. We compared the four (4) common visible-near infrared bands with the eight (8) band WorldView-2 image. The 8-band WorldView-2 image yielded higher overall accuracy of 86.90% (kappa = 0.82) than the common 4 band image which yielded an overall accuracy of 74.64% (kappa = 0.63) in pixel-based classification. We further compared the vegetation indices in object-based classification, which were derived from four common bands, with those that are derived from WorldView-2. The Enhanced Vegetation Index (EVI) yielded the highest overall accuracy in the category of common indices (85.59% at kappa = 0.79), while the modified Plant Senescence Reflectance Index (mPSRI) showed the highest overall accuracy (93.69%) in the category of indices derived from an eight band WorldView-2 image in object-based classification. This study shows the utility of WorldView-2 imagery in enhancing the common 4 band imagery and eventually improving the delineation of forest gaps.

Keywords*: Canopy gaps, invasive species, WorldView-2, spatial resolution, EVI, mPSRI*

Malahlela, O.E., Cho, M.A., Mutanga, O (in preparation). Mapping forest canopy gaps in an indigenous coastal forest of Dukuduku in KwaZulu-Natal, using WorldView-2 imagery. *International Journal of Remote Sensing*

2.2 Introduction

Subtropical coastal forests in South Africa are rich in biodiversity (Geldenhuys, 1989). Over the years, forests have been fragmented into patches of various sizes. The fragmentation has resulted from anthropogenic activities such as subsistence farming, commercial agriculture and human settlement development (Fourcade, 1889; Geldenhuys, 1989). Some of the patches are intensively managed e.g. the Dukuduku coastal forest (Van Gils et al., 2006). However, the sustainability of indigenous biodiversity in the remnant patches is threatened by the presence of alien invasive species (Van Gils et al., 2006; Moore, 2004). The alien invasive species take advantage of forest gaps that occur within the patches for their establishment. Forest gaps can be formed from tree-fall (Kupfer and Runkle, 1996; Brokaw et al 1982), uprooting or timber harvesting (Suarez et al., 1997) or any catastrophic disturbance (Brokaw, 1982a; Whitmore, 1989). Naturally, in a stable tropical forest, forest gaps are closed up by the regenerating indigenous species through a process of succession (Orians, 1982). However, in South Africa, forest gaps in coastal forests may be invaded by species such as *Chromolaena odorata* which is a very common invader (Weiss and Noble, 1984; Goodall and Erasmus, 1996). Therefore, the delineation of forest gaps is crucial for management geared towards eliminating invasive species.

The delineation of forest gaps was previously done through field surveys (Brokaw and Grear, 1991). The applicability of field based methods was only limited to areas that are easily accessible, with homogeneous terrain and mostly in savannah environments (Runkle, 1982). Identifying forest gaps in subtropical forest through field surveys is practically impossible for larger and wider areas. To address this challenge, remote sensing techniques have been used as a more reliable alternative to delineate forest gaps over a large area. These techniques have benefit in that they reduce the time and effort needed to cover an extensive area (Woodcock et al., 2001). The detection of forest gaps has been studied previously using Landsat imagery with a spatial resolution of 30 meters (Negrón-Juárez, 2011; Asner et al., 2004). The limitation of this coarse resolution sensor lies in its inability to map canopy gaps less than the 30 m pixel size (Clark et al., 2004). The use of high resolution multispectral sensors such as *Système Pour l'Observation de la Terre* (SPOT) and IKONOS has mitigated the spatial resolution problem by improving accuracy in vegetation studies (Clark et al., 2004). However, Knipling (1970) and recently Chen et al. (2009) have documented that these multispectral sensors suffer from a saturation problem in the visible-near infrared regions in dense vegetation. This problem could potentially make discrimination between tree canopies

and vegetated gaps in closed canopy coastal forests difficult (Fig. 2) (Weiss and Baret, 1999). Recently, high resolution hyperspectral data were utilized to mitigate the saturation problem common in common multispectral sensors (Treitz et al., 2003; Ustin and Trabuco, 2000). The utility of the red edge band present in hyperspectral sensors has proven to solve the saturation problem, e.g. the red edge Normalized Difference Vegetation Index (NDVI) has improved the estimation of vegetation biomass (Mutanga and Skidmore, 2004; Smith et al., 2004). However, the use of high resolution data has not been fully explored due to the high costs associated with acquiring these data (Asner et al., 2004). Some studies have also pointed out that hyperspectral data may suffer from data redundancy for specific applications (Cho et al., 2012; Mutanga et al., 2012).

The development of high spatial and spectral resolution multispectral data sensors such WorldView-2 (Ozdemir and Karnieli, 2011) and RapidEye (Ramoelo et al., 2012) has created new opportunities for diverse vegetation studies. The red edge band present in these sensors (Fig. 2) has been successfully used to estimate grass nitrogen (Ramoelo et al., 2012) and biomass in closed canopy forest (Mutanga et al., 2012). The question that arises is whether the presence of the red edge band in WorldView-2 can provide improved discrimination of forest gaps in a closed canopy coastal forest when compared to the common red, green, blue and NIR bands present in common sensors such as SPOT, IKONOS or Landsat?

In addition, canopy gap delineation requires classification techniques that will aid in separating forest gaps from the rest of forest canopies. A number of studies have delineated forest gaps using common pixel-based parametric classifiers such as maximum-likelihood and spectral angle mapper classifiers (Fox et al., 2000; Negrón-Juárez et al., 2011; Betts et al., 2005). Pixel-based classification methods have their own short-comings when applied to closed canopy forests. These techniques only consider spectral information and not the geometry and size of individual forest gaps (Mallinis et al., 2008; Kim et al., 2009). The question is whether object-based image analysis can assist in minimizing the short-comings of pixel-based classifications in delineating forest gaps, and thereby improve on the classification accuracies(as shown in fig.3)? An object-based classifier has advantages in that, although being a non-parametric classifier, it requires less computational space compared to methods such as Artificial Neural Network and Random Forest (Blaschke and Strobl, 2001).

The aims of this study are:

a) To test the utility of WorldView-2 multispectral bands in delineating forest gaps, when compared to common visible-near infrared bands common in common sensors.
b) To determine the best vegetation indices for delineation of forest gaps in closed canopy coastal forest using object-based classification
c) To investigate the performance of an object-based classification technique over pixel-based classification methods for delineating forest canopy gaps.

The delineated forest gaps were expected to contain characteristics relevant to the prediction of invasive species. These characteristics include gap perimeter and gap size.

2.3. Methods

2.3.1 Study area

The study was undertaken in Dukuduku coastal forest located near St. Lucia, north eastern part of KwaZulu Natal, South Africa. It is located within the Mtubatuba Local Municipality between the geographical coordinates of 28°38‘33”S and 32°31’67” E (fig. 4). The forest covers a land area of about 3 200 hectares.

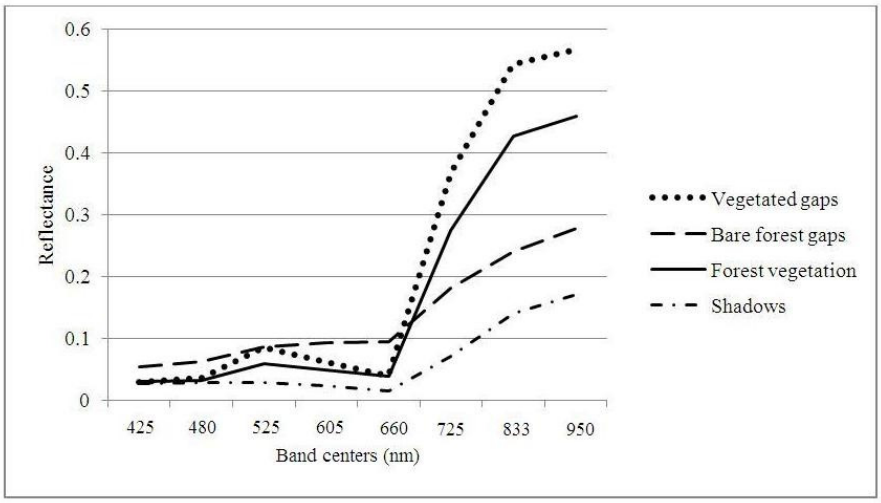

Fig.2: Spectral profile of five averaged spectra of four classes from WorldView-2 imagery of the Dukuduku forest. This figure shows that four forest classes are distinguishable by observing their spectral profiles.

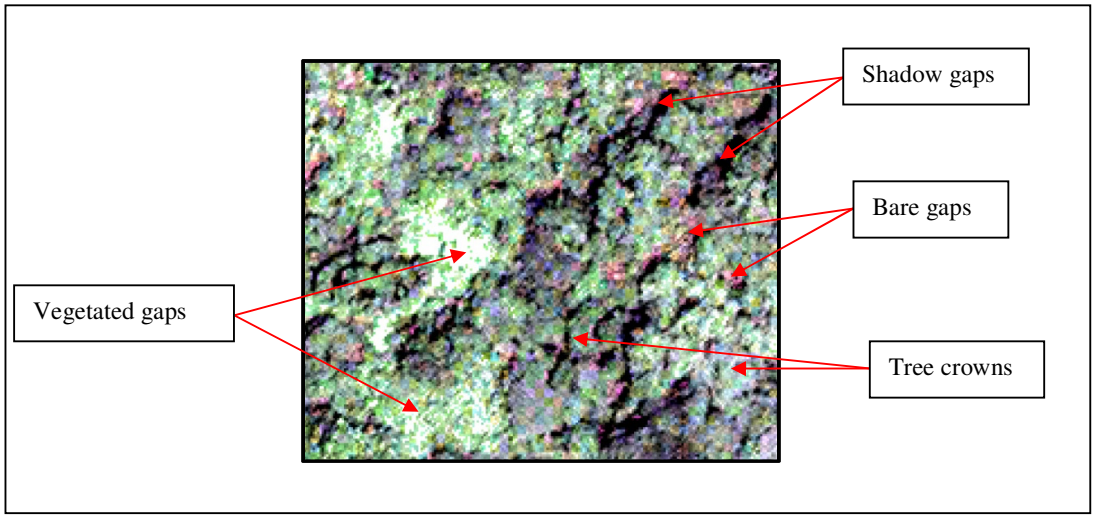

Fig.3: WorldView-2 imagery subset showing canopy gaps and the surrounding tree canopies

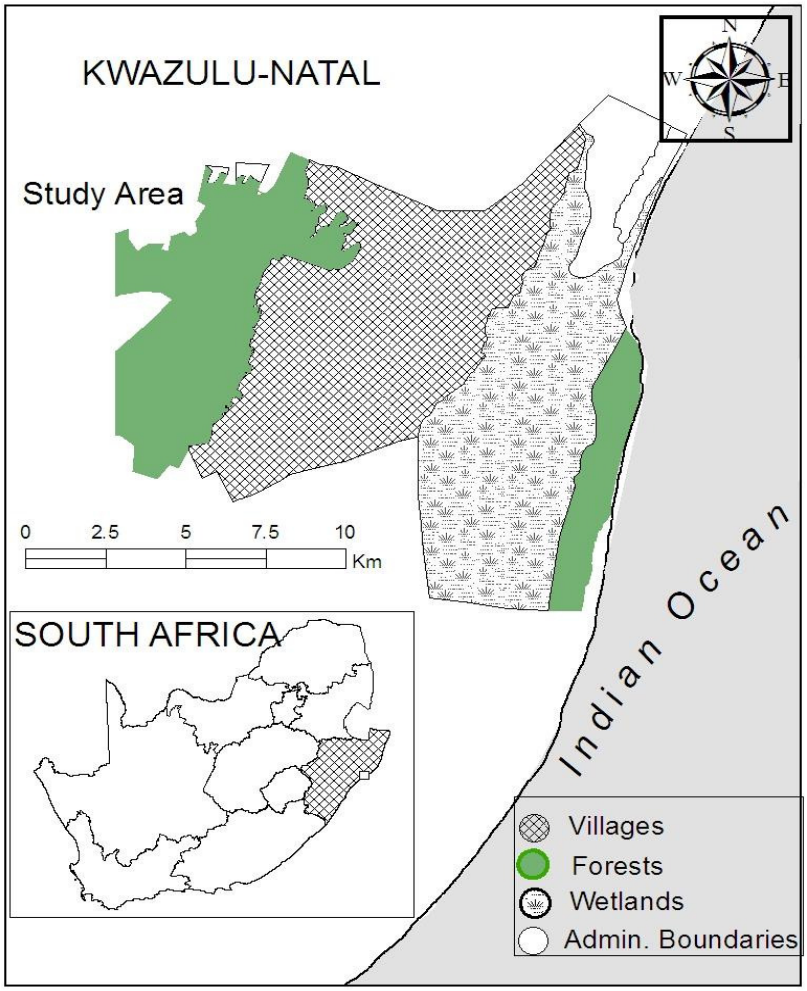

Fig. 4 The location of the study area in KwaZulu-Natal.

The area was chosen for the study because it is the largest of the remaining patches of indigenous forest on the north-eastern coastal shoreline of KwaZulu-Natal. This area is one of the largest forest patches that are subjected to clearance for agricultural and settlement activities. Alien species invasion especially by *Chromolaena odorata* poses a major threat to the indigenous forest in this area. This forest is surrounded by sugar plantation farms, *Eucalyptus* plantations and villages that practise a different farming practice, usually subsistence farming. According to Van Wyk et al. (1996), the topography of the study area comprises of a few minor north-south-trending dune ridges, which occur on a low plateau that rises to a maximum of 60 m above the mean sea-level. The soils in this area are mainly

deep and predominantly derived from recent wind-deposited sands, with high leaching and poor nutrient status (Luwum, 2002).

The climate of KwaZulu-Natal is subtropical, with high summer precipitations and high temperatures of over 33°C (between September and April). Winters are generally cooler (below 8°C), with the annual sea surface temperatures of 15°C. The study area receives an annual rainfall of about 1400 mm (Le Roux, 2013).

2.3.2 Image data acquisition and processing

The WorldView-2 image with 8 multispectral bands (Table 1) acquired on the 1st December 2010 was used for the study. WorldView-2 has four new additional bands that are not present in well-known sensors such as SPOT, IKONOS or Landsat. This sensor has spectral bands that are strategically located to aid in vegetation analysis. The spectral bands have wavelength ranges of 400 – 450 nm (absorbed by chlorophyll), 450 – 510 nm (absorbed by chlorophyll), 510 – 580 nm (sensitive to plant health), 585 – 625 nm (absorbed by carotenoids – detects 'yellowness' of vegetation), 630 – 690 nm (absorbed by chlorophyll), 705 – 745 nm (sensitive to vegetation health), 770 – 895 nm (sensitive to leaf mass and moisture content), 860 – 1040 nm (sensitive to leaf mass and moisture content) (Ustin et al., 2009). The WorldView-2 (WV-2) imagery was geometrically corrected by the supplier (Updike and Comp, 2010). To assess the accuracy of geometric correction, coordinates of some iconic points on the ground, including road junctions and isolated tree canopies were extracted from the image and loaded onto a handheld GPS.

With the help of GPS, the uploaded points were quite accurately located on the ground to within 2 meters. Atmospheric correction was carried out using ATCOR 2/3 version module (developed and distributed by ReSe Applications). An ATCOR2/3 is based on a MODTRAN 5 code (Berk et al., 1998). A MODTRAN 5 code (MODerate resolution atmospheric TRANsmission) is an algorithm designed to model atmospheric propagation of electromagnetic radiation by calculating the databases of atmospheric look-up tables for the spectral regions of between 0.2 and 100 µm (Berk et al., 1998) .

Table 1
WorldView-2 bands and their respective centers compared to bands present in SPOT and Landsat.

Band Name	**Wavelength (nm)**	**Band Centers (nm)**	**Present in common sensors**	
			SPOT	***Landsat***
Coastal Blue	400-450	425	No	No
Blue	450-510	480	No	Yes
Green	510-580	545	Yes	Yes
Yellow	585-625	605	No	No
Red	630-690	660	Yes	Yes
Red-Edge	705-745	725	No	No
Near Infrared-1	770-895	833	Yes	Yes
Near Infrared-2	860-1040	950	No	No

The atmospheric conditions specified in the ATCOR software for this image processing was the 'tropical rural' conditions. Figure 5 shows the stages from image analysis to eventual gap delineation using WorldView-2 imagery of the Dukuduku forest.

2.3.3 Field data collection

Two field data collection trips were carried out in order to record data on forest gaps, invasive plant species and the surrounding indigenous vegetation. The first field data collection trip was undertaken between 24 July 2011 and 4 August 2011, while the second one was from the 21 October to 2 November 2011. These dates were primarily dictated by the condition of the atmosphere to avoid rainy weather at the coast. Line transects were randomly pre-selected across the entire forest, which represented the general trend of vegetation characteristics and cover in the forest (Eberhardt, 1986; Battles et al., 1996). The data were collected along these transects (fig. 5), which included vegetated forest gaps (with/without invasive plant species), bare forest gaps and the individual tree crowns of forest vegetation.

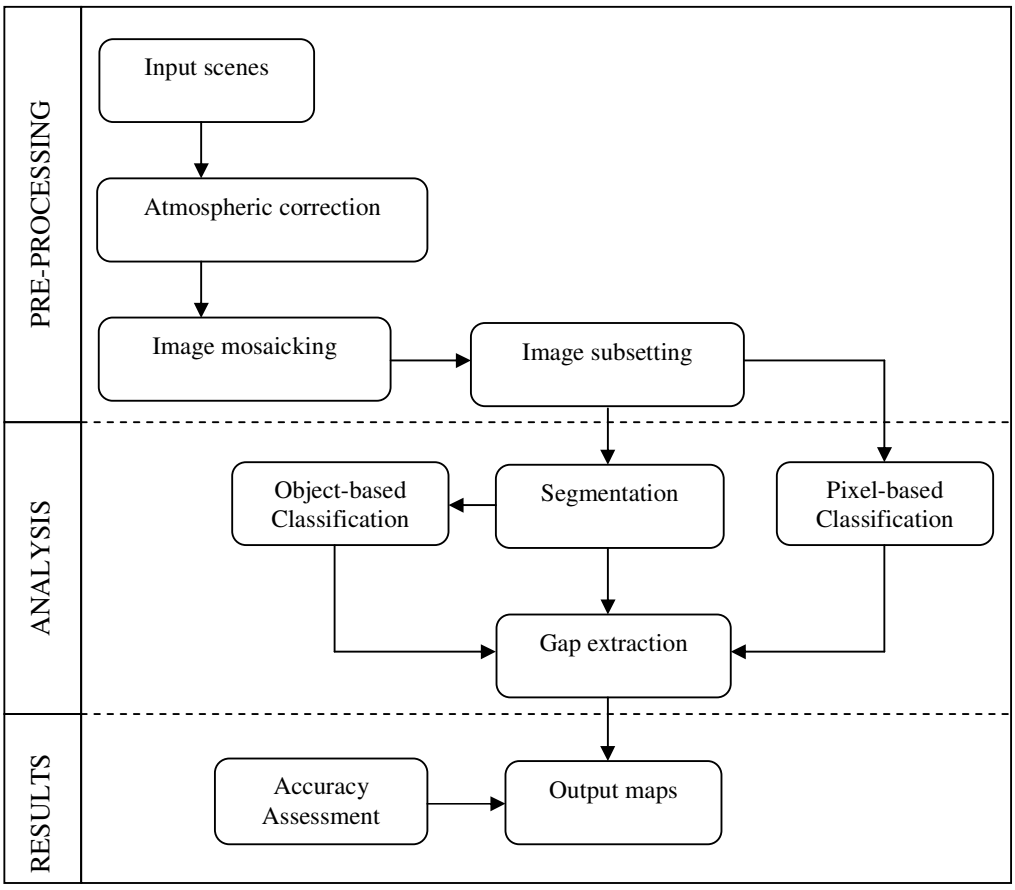

Fig. 5 A workflow used for the delineation of forest gaps using WorldView-2 in the Dukuduku coastal forest

A standard Global Positioning System (GPS) named Garmin Vista eTRax™, with maximum spatial accuracy of 4 meters, was used to record the location of each forest gap and the surrounding vegetation type (Fig. 6). A total number of 276 samples were collected. The data were randomly split into 60% calibration and 40% for validation as seen in Table 2. The calibration dataset was used for training the classifiers. The validation dataset was used to assess the accuracy and the reliability of the classification techniques.

Table 2
Number of training and validation points per class type.

Class	**Training**	**Validation**	**Total**
Bare gaps	41	27	68
Vegetated gaps	29	19	48
Shadows	28	19	47
Other vegetation	67	46	113
Total	165	111	276

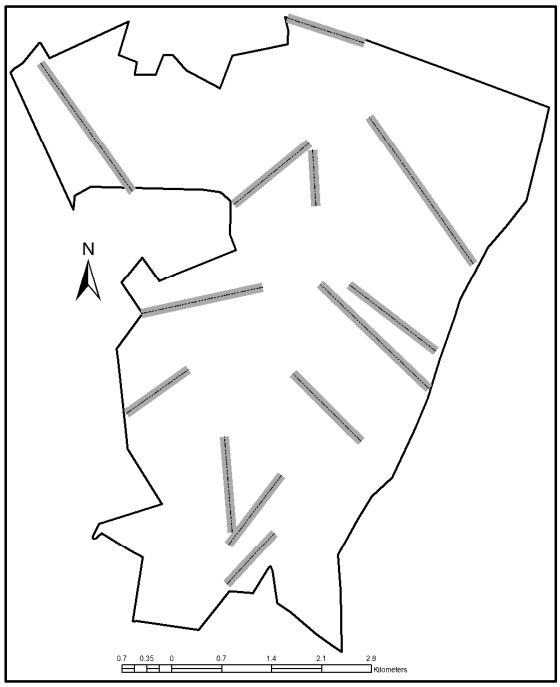

Fig. 6 The distribution of line transects (grey lines) in the Dukuduku coastal forest.

2.3.4 Image classification

Two approaches of image classification were tested for this study, namely pixel-based classification and object-based image analysis. For pixel-based image analysis, classification methods such as maximum likelihood (MLC), parallelepiped (PPC) and minimum distance (MDC) were explored to determine the best commonly used pixel-based classifier for forest gap delineation. In object-based analysis, a multi-resolution segmentation algorithm was explored for creating image objects at different scale parameters (10, 25, and 35). The threshold values from computed vegetation indices were used to discriminate forest vegetation into separate classes.

2.3.4.1 Pixel-based classification

Three pixel-based classification methods were tested for the study, namely, minimum distance, maximum likelihood and parallelepiped classifiers. The minimum distance classifier is based on the minimum distance decision rule that calculates spectral distance of the measurement vector for the candidate pixel and the mean vector of each sample. The method

further assigns the candidate pixel to the class having minimum spectral distance (Perumal and Bhaskaran, 2010). This method was applied for classifying forest into four main classes (i.e. bare forest gaps and surfaces, shadows, vegetated forest gaps, other forest vegetation).

Maximum likelihood classifier is based on a normalized (Gaussian) estimate of the probability density function of each class. It is known to be the most powerful classification method when accurate training data is provided and one of the most widely used algorithm (Zhou and Robson, 2001). Parallelepiped is a widely used decision classifier based on less complex Boolean operations of "and/or" logic. Digital values from each pixel of the multispectral imagery are used to produce an n-dimensional mean vector, and consequently consider the standard deviations of the candidate pixel to the mean (Lillesand and Keifer, 1993).

2.3.4.2 Object-based classification

Object-based image analysis (OBIA) does not operate on a single pixel, as in the case of pixel-based classification. The process of classification begins with image segmentation where similar pixels are merged together using homogeneity criteria such as spectral similarity, weight or compactness (Baatz et al., 2004). Performance of classification in object based relies on the quality of individual image segments and the accuracy of the segmentation process. A multi-resolution segmentation algorithm was used to begin the segmentation process, where three scale parameters (10, 25, and 35) were tested. The scale parameter of 10 was selected because the objects created were not very different in size and shape from what was observed in the field, and the accuracy of class discrimination decreased with increasing scale parameter (fig.7). A multi-resolution algorithm is embedded in eCognition software, which is an object-based processing program made available in 2000 from Definiens Imaging GmbH (Blaschke and Strobl, 2001). Vegetation indices were calculated in eCognition and were used to discriminate four (4) forest classes, using individual index's decision tree, where thresholds were defined at each level to allocate segmented objects to a particular class.

We tested established vegetation indices that were derived from spectral bands present in common satellites such as Landsat and SPOT, and those that can be derived from WorldView-2 new bands for delineation of forest gaps. Vegetation indices were selected from those that were sensitive to broadband greenness, narrowband greenness and plant senescence (Asner et al, 2002). Tables 3 show vegetation indices that are derived from

common Red, Green, Blue and Near-Infrared bands, and also the vegetation indices derived from new WV-2 bands.

2.3.5 Accuracy Assessment

Classification accuracies were used to assess the reliability of the results; namely, producer, user and overall accuracies. Producer accuracy is derived from calculating the total number of correctly classified cases in one class divided by the total number of cases of that class as indicated by reference data (Congalton, 1991). The user accuracy is derived from calculating the total number of correctly classified cases of one category divided by the total number of cases classified in that category (Story and Congalton, 1986). Finally, overall accuracy is computed by dividing the number of correctly classified cases by the total number of cases in the error matrix. Error matrix tables were computed as part of the accuracy assessment procedure. The procedure of computing error matrices is a very effective way to present accuracy in that accuracies are described along with both errors of inclusion (commission errors) and errors of exclusion (omission errors) present in the classification (Congalton, 1991).

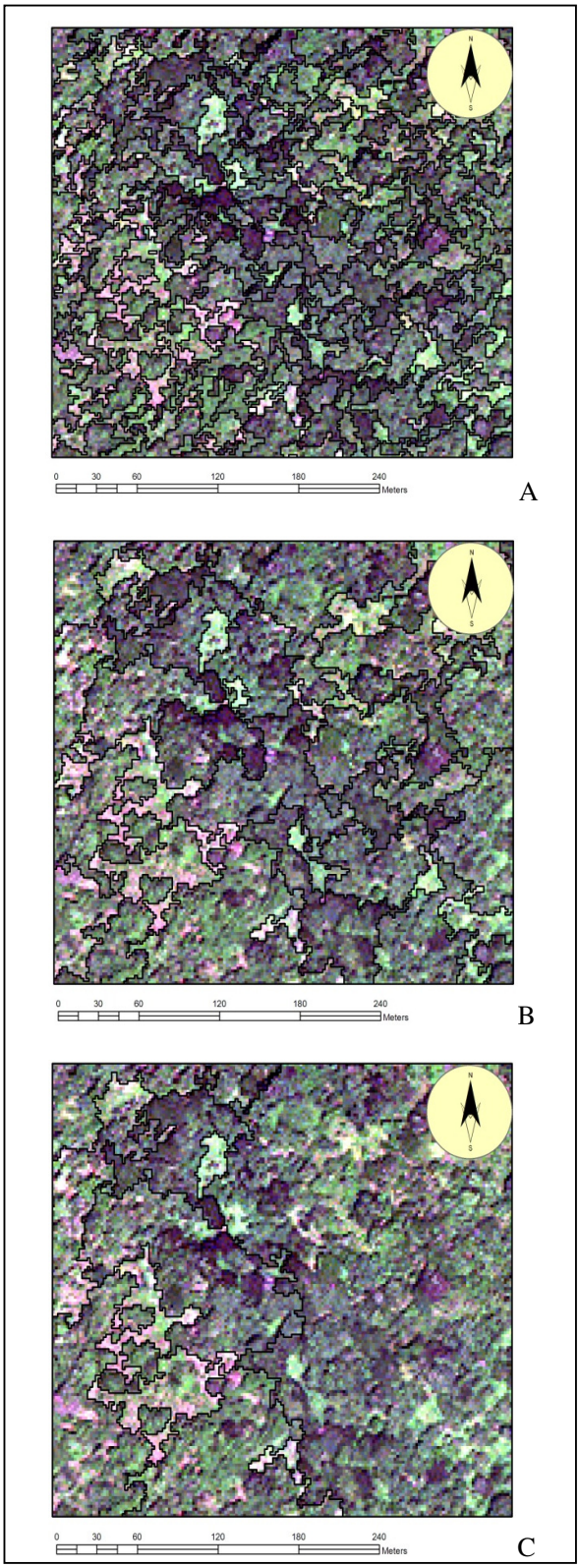

Fig. 7: Segmentation of WorldView-2 image of Dukuduku forest at different scale parameters (A = 10, B = 25 and C = 35).

Tables 3

Established vegetation indices derived from (a) common sensors and those derived from (b) WorldView-2

(a)

	Index	Equation	Reference
Common Sensors (Landsat 7/SPOT 5)	Normalized Difference Vegetation Index ($NDVI_{660}$)	$\mathrm{NDVI}_{660} = \frac{\rho_{NIR} - \rho_{Red}}{\rho_{NIR} + \rho_{Red}}$	Jackson et al. (1983)
	Enhanced Vegetation Index (EVI)	$EVI = 2.5\left(\frac{\rho_{NIR} - \rho_{Red}}{\rho_{NIR} + 6\rho_{Red} - 7.5\rho_{Blue} + 1}\right)$	Huete et al.(1997)
	Atmospherically Resistant Vegetation Index(ARVI)	$ARVI = \frac{\rho_{NIR} - (2\rho_{Red} - \rho_{Blue})}{\rho_{NIR} + (2\rho_{Red} - \rho_{Blue})}$	Kaufman and Tanre (1992)
	Green Normalized Difference Vegetation Index ($NDVI_{545}$)	$NDVI_{545} = \frac{\rho_{833} - \rho_{545}}{\rho_{833} + \rho_{545}}$	Gitelson and Merzlyak. (1994)

(b)

	Index	Equation	Reference
WorldView-2 Sensor	Modified plant Senescence Reflectance Index (mPSRI)	$mPSRI = \frac{(\rho_{660} - \rho_{480})}{\rho_{725}} * 1.5$	Merzlyak et al.(1999)
	Normalized Pigment Chlorophyll Index (NPCI)	$NPCI = \frac{\rho_{660} - \rho_{425}}{\rho_{660} + \rho_{425}}$	Peñuelas et al. (1995)
	Red Edge Normalized Difference Vegetation Index ($NDVI_{725}$)	$NDVI_{725} = \frac{\rho_{835} - \rho_{725}}{\rho_{835} + \rho_{725}}$	Gitelson and Merzlyak (1994)
	Yellowness Index (YI)	$\mathrm{YI} = \frac{\rho(\lambda_{-1}) - 2\rho(\lambda_0) + \rho(\lambda_{+1})}{(\lambda_{660} - \lambda_{605})^2}$	Adams et al.(1999)

	Index	Equation	Reference
WorldView-2 Sensor	Near Infrared Normalized Vegetation Index ($NDVI_{NIR}$)	$NDVI_{NIR} = \frac{\rho_{NIR1} - \rho_{NIR2}}{\rho_{NIR1} + \rho_{NIR2}}$	Tested for the study
	Yellow Normalized Difference Vegetation Index ($NDVI_{605}$)	$NDVI_{605} = \frac{\rho_{NIR} - \rho_{605}}{\rho_{NIR} + \rho_{605}}$	Tested for the study

2.3.6 Comparing Classifier Performance

In order to compare the performance among the classifiers, a McNemar's test was applied on the results of each classifier against another. The McNemar's test was used to test for the performance of the classifiers since the same samples were used for classification tests, and were therefore not independent as would be required for the Kappa difference test (Foody, 2004). The McNemar's test is preferable since it is a parametric test and very simple to understand. The test is based on a chi-square (χ^2) statistic, computed from two error matrices as follows:

$$\chi^2 = \frac{(f_{12} - f_{21})^2}{f_{12} + f_{21}} \qquad \text{Eq: 1}$$

where f_{12} denotes the number of cases that are wrongly classified by classifier 1 but correctly classified by classifier 2, and f_{21} denotes number of cases that are correctly classified by classifier 1 but wrongly classified by classifier 2. Additional f_{11} and f_{22} were included to indicate the number of cases wrongly classified by both classifiers, and the number of cases correctly classified by both classifiers, respectively.

2.4 Results

2.4.1 Pixel-based classification

Maximum likelihood classifier showed the highest overall classification accuracies (86.90%) when compared to minimum distance (64.86%) and parallelepiped (65.76%) classifiers. It showed the highest average producer and user accuracies for all four classes (86.33% and 87.54%, respectively) when compared to minimum distance (66.19% and 66.60%, respectively) and parallelepiped (55.91% and 78.30%, respectively). Maximum likelihood classifier also showed higher overall and average user accuracies (86.90% and 86.33%, respectively) for the 8-band WorldView-2 imagery when compared to the spectrally resampled 4 band image similar to SPOT, IKONOS and Landsat (74.64% and 70.83%, respectively) as seen in table 4.

2.4.2 Object-based classification

The results of vegetation indices were divided into two groups: (i) vegetation indices that can be derived from common sensors (typical Red, Green, Blue and Near-Infrared bands) of WorldView-2, and (ii) vegetation indices that can be derived from the 8-band WorldView-2 imagery. Amongst the vegetation indices derived from common sensors, the enhanced vegetation index (EVI) computed from common R.G.B and NIR bands yielded the highest average producer (85.07%), average user (79.73%) and overall classification accuracies (85.59%) on all forest classes. On the contrary, the atmospherically resistant vegetation index (ARVI) yielded the lowest average user and overall classification accuracies (60.42% and 67.57%, respectively). The yellow normalized difference vegetation index ($NDVI_{605}$) yielded the lowest average producer accuracy (68.23%) for all forest classes (appendices B).

Amongst the indices derived from WorldView-2 bands, the modified plant senescence reflectance index (mPSRI) showed the highest average producer (92.10%) and average user accuracy (93.50%) for all classes as well as the highest overall classification accuracy (93.69%) (Table 4). On the other hand a yellowness index (YI) yielded the lowest average producer (58.00%), average user accuracy (58.72%) and overall classification accuracy (60.36%) as seen in appendices B. The difference between high performing vegetation index from common bands (overall classification accuracy of 85.59 %) and that from WorldView-2 bands (overall classification accuracy of 93.69%) is 8.1%. Fig. 8 shows the results of the

delineated gaps and the confusion matrix is shown by Table 6. The mPSRI showed average producer accuracy of 90.25 % and average user accuracy of 90.26 % for forest gaps.

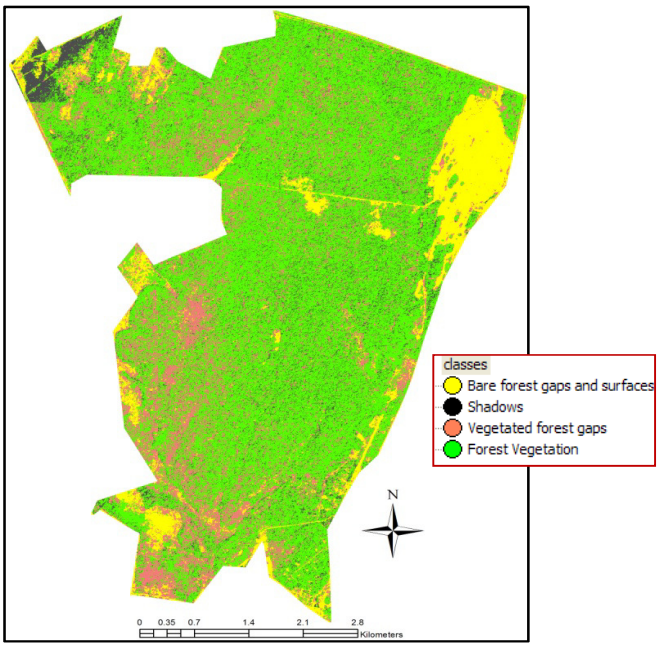

Fig. 8 Delineated forest gaps resulting from mPSRI in object-based classification

Table 4
Classification accuracies from pixel-based and object-based methods (PA = Producer accuracy, UA = User Accuracy)

Class name	Pixel-based classification MLC (4 bands)		Pixel-based classification MLC (8 bands)		Object-based classification (EVI)		Object-based classification (mPSRI)	
	PA (%)	UA (%)	PA (%)	UA (%)	PA (%)	UA (%)	PA (%)	UA (%)
Bare gaps	83.5	73.6	95.4	97.4	79.4	100	96.2	96.3
Vegetated gaps	73.2	61.3	84.1	90.4	78.5	57.9	84.2	84.2
Shadow gaps	67.1	62.6	84.6	81.2	92.3	63.2	90.4	100
Others	71.2	85.6	81.0	81.0	90.0	97.8	97.7	93.5
Overall accuracy (%)	74.64		86.90		85.59		93.69	

Table 5
Comparison of the classifier performance for both pixel-based and object-based classifiers using McNemar's test

Models Compared	f_{11}	f_{12}	f_{21}	f_{22}	**Total**	**chi-sq. ($\chi 2$)**	**p value**	**df**
mPSRI vs. MLC (8 bands)	7	8	0	96	111	8	<0.05	1
mPSRI vs. MLC (4 bands)	7	26	0	78	111	26	<0.05	1
mPSRI vs. EVI	7	10	4	90	111	7.6	<0.05	1
MLC (8 bands) vs. MLC (4 bands)	10	23	0	78	111	23	<0.05	1
MLC (8 bands) EVI	10	10	1	90	111	9.1	<0.05	1
MLC (4 bands) vs. EVI	20	2	11	78	111	51.5	<0.05	1

Table 6
Confusion matrix resulting from mPSR Index in object-based image analysis

		Reference Image					
	Class	Bare gaps	Vegetated gaps	Shadows	Others	Total	*User Accuracy*
Classified Image	Bare gaps	26	1	0	0	27	96.30
	Vegetated gaps	1	16	1	1	19	84.21
	Shadows	0	0	19	0	19	100.00
	Others	0	2	1	43	46	93.48
	Total	27	19	21	44	111	
	Producer Accuracy%	96.29	84.21	90.48	97.73		
	Kappa Index					0.91	
	Overall Accuracy					93.69	

Table 5 shows McNemar's test results with the number of cases correctly and incorrectly classified by pixel based methods (8 band WorldView- image and common 4 band image), and object-based methods (Enhanced Vegetation Index and modified Plant Senescence Reflectance Index). The results showed that there was a statistical difference between pixel-based and object-based classification techniques. All comparisons showed statistical difference amongst each other at $\rho < 0.05$ and at 1 degree of freedom. Table 7 shows the results of three (3) best vegetation indices derived from (i) common R.G.B and NIR bands common in Landsat, and (ii) WorldView-2 sensor.

Table 7
Comparison of classification results obtained from vegetation indices derived from common sensor and those from WorldView-2 imagery. (PA= mean producer accuracy, UA= mean user accuracy, OA= overall accuracy)

	Index	**PA (%)**	**UA (%)**	**OA (%)**
Common R.G.B, NIR Indices	EVI	85.0	79.7	85.6
	$NDVI_{545}$	83.5	80.7	84.7
	$NDVI_{660}$	75.1	73.8	82.9
New WorldView-2 Indices	$NDVI_{725}$	75.1	80.7	82.9
	mPSRI	92.1	93.5	93.7
	NPCI	73.2	74.3	78.4

2.5 Discussion

Canopy gaps form an important part of forests and have been mapped using different methods (Runkle, 1982: Emborg, 1998; Vepakomma et al., 2008) but rarely in subtropical forests (Brokaw, 1985a). Most of the studies focused on delineating forest gaps from combined optical and hyperspectral data (Hodgson and Bresnahan, 2004). To the best of our knowledge, high resolution multispectral data alone has not been used for delineating forest canopy gaps in closed canopy environment. Findings from this study show the possibility of using high spatial resolution WorldView-2 imagery for delineating forest gaps in the subtropical forest environment. Higher classification accuracies were achieved from an 8-band WorldView-2 image when compared to the common 4 band imagery (red, green, blue and near infrared bands) similar to those found in SPOT, IKONOS and Landsat. In addition, the best three highest performing indices derived from WorldView-2 imagery (NPCI, mPSRI and $NDVI_{725}$) yielded the highest average user accuracy (82.83%) for all forest classes (Table 7) compared to the three best performing indices derived from common sensors (EVI,$NDVI_{545}$ and $NDVI_{660}$) (78.07%) in object-based image analysis. This evidence supports the assertion that the utility of WorldView-2 sensor provides improved estimates of vegetation biophysical characteristics in subtropical environments (Mutanga et al., 2012; Cho et al., 2012).

The maximum likelihood classifier applied on a spectrally resampled 4-band imagery, common in SPOT, IKONOS and Landsat, showed a drop in average user and overall classification accuracies (from 86.33% to 70.83%, and from 86.90% to 74.64% respectively), which is an indication that new WorldView-2 bands provide spectral enhancements to the common RGB and NIR bands (Mutanga et al., 2012; Cho et al., 2012; Ozdemir and Karnieli, 2011). This indicates that WorldView-2 bands can improve on the discrimination of forest gaps from other forest classes. The pixel-based overall classification accuracy resulting from WorldView-2 bands is 15.50% higher than the overall classification accuracy derived from common RGB and NIR bands. This evidence also highlights the spectral saturation that poses a major challenge when using common bands (Cho et al., 2008) and shows that the presence of new WorldView-2 bands can minimize this problem.

The mPSRI which is derived from new bands of WorldView-2 yielded the highest overall classification accuracy than all the selected indices. The mPSRI index is derived from a plant senescence reflectance index proposed by Merzlyak et al. (1999). Although this index was initially proposed to estimate the stage of leaf senescence and fruit ripening, our study indicates that it can also be used to delineate forest gaps in closed canopy forest. The performance of this index can be attributed to the background of canopy gaps, whose spectral behaviour is similar to senescing vegetation areas. Additionally, we have observed the increased average user and overall classification accuracies of red edge NDVI over the common NDVI. The saturation problem that is prevalent in common sensors is minimized when the red edge band is used in vegetation indices such as NDVI, and this characteristic was crucial for our study since the confusion between vegetated gaps and tree crown was minimized (Mutanga and Skidmore, 2004). This confirms our hypothesis that separability of forest gaps from forest tree crowns can be increased by using indices that are derived from WorldView-2 than those derived from common sensors.

The EVI which is derived from common RGB and NIR bands yielded the highest overall accuracy for the study compared to all other selected indices under this category. This is an index that has been used in vegetation studies, and it is known for its sensitivity to canopy's structural variations (Jiang et al., 2008). This index was particularly important since the discrimination of canopy structure of vegetated gaps from the surrounding forest canopies is a central focus of this study. On the contrary, the ARVI yielded the lowest average user and overall classification accuracies for gap delineation. The ARVI is an index designed to correct for atmospheric scattering of the red reflectance by using the blue band (Kaufman and Tanre, 1996). WorldView-2 has an advantage over common sensors in that it possesses a high spatial resolution (2 m multispectral), and this characteristic plays a significant role considering that gap sizes can be any 'hole' in a forest of 2 meters in diameter (size) and height (length) (Brokaw et al., 1982). Although hyperspectral datasets have high spatial and spectral resolution, they have not been used extensively due to high cost associated with data acquisition. The development of high spatial resolution sensors such as WorldView-2 with a red edge band, similar to hyperspectral, provides an affordable alternative for forest gap mapping. The importance of the red edge band in WorldView-2 has also been recognised in another application at the same study area (Mutanga et al., 2012).

Findings from the study suggest that pixel based classification (PIBC) approach can assist in delineating forest gaps. However, not all the methods in this approach resulted in high classification accuracies for the delineation of forest gaps in the study area. Maximum likelihood classifier (MLC) still offers highly accurate results over its parametric pixel-based counterparts. Our results confirm findings by Borak and Strachler (1999) which showed that MLC yielded the highest classification accuracies than PPC and MDC for classification of land cover using a MODIS-like data. In the PIBC category, although MLC showed the highest classification accuracies than all other parametric classifiers, it was limited by its consideration of spectral information only while an object based classification additionally considered the weight, shape and size of objects (Yan et al., 2007). Vegetation indices have long been used in remote sensing for assessing plant health, biomass, phenology and cover (Kerr and Ostrovsky, 2003). For this study the vegetation indices were derived from WorldView-2 imagery in object-based image analysis. The object-based image analysis (OBIA) results were not significantly different from the ones derived from MLC (overall accuracy of 93.69% and 86.90%, respectively), and therefore, integrating these methods may increase delineation accuracy. However, results derived from OBIA provided a basis for the derivation of gap size and perimeter required for further invasive species habitat analysis (Saura, 2001).

One of the most important factors to consider in OBIA is the scale parameter. Our study has shown that the lower scale parameter (10) was efficient in assisting with creating image objects that were classified into their respective classes. It was found that higher scale parameters tend to create larger objects after segmentation process and this makes it impossible to delineate forest gaps, without including adjacent shadow and tree canopies. The multi-resolution segmentation was one of the ways that was explored for our study, in order to utilize spectral information. However there are other methods that incorporate spectral information that were not tested for the study. These methods include textural and contextual methods that have shown to be efficient when applied to high resolution imagery such as IKONOS (Mallinis et al., 2008).

2.6 Conclusion

Forest gaps were successfully delineated using both pixel-based and object-based classification techniques. The following conclusions were drawn from the study:

- The use of 8-band WorldView-2 imagery increases classification accuracies (average producer, user and overall) for delineating forest canopy gaps when compared to the common VNIR bands present in SPOT, IKONOS and Landsat.
- Vegetation indices derived from new WorldView-2 red-edge band ($NDVI_{725}$ and mPSRI) yielded higher average user accuracy than those that are derived from common sensors.
- The mPRSI in object-based image analysis yielded the highest overall accuracy in the study amongst all classification methods.

Chapter Three

Integrating Environmental Data and Worldview-2 Data to Map the Probability of Occurrence of *Chromolaena odorata* in Forest Gaps, Dukuduku Coastal Forest in KwaZulu-Natal, South Africa[2]

3.1 Abstract

Indigenous forests in South Africa are rich in native biodiversity. However, the native biodiversity richness is threatened by the presence of invasive species that may take advantage of forest gaps. Mapping the probability of occurrence of invasive species in forest gaps is therefore crucial for forest management. Our study explored the utility of WorldView-2 imagery (with 8 bands) for mapping the probability of occurrence of invasive *Chromolaena odorata* in forest gaps of Dukuduku Forest, South Africa. The WorldView-2 bands were integrated with ancillary environmental data for mapping *Chromolaena odorata* presence and absence in forest gaps. Results of the study show that the coastal (λ_{425} nm) and the near-infrared1 (λ_{833} nm) bands were significantly positively related to the presence and absence of invasive species. The yellow (λ_{605} nm) and the near-infrared2 (λ_{950} nm) bands and the red edge NDVI ($NDVI_{725}$) were negatively correlated with the presence and absence of *Chromolaena*. Ancillary environmental data yielded a deviance (D^2) of 0.12 (12%), while the WorldView-2 bands alone yielded a D^2 of 0.20 (20%). An integrated model (ancillary environmental data and WorldView-2 data) yielded a D^2 of 0.42, which means that 42% of variability in the presence and absence of *Chromolaena odorata* in forest gaps can be explained by an integrated model. A 2x2 error matrix table and the receiver operating characteristic (ROC) curves from an independent validation dataset were used to assess mapping accuracy. About 86.8% of the predicted cases were correctly classified at the probability threshold of 0.5. The results suggest that integrating WorldView-2 data with ancillary environmental data increases the accuracy of invasive species mapping.

Keywords*: Mapping, remote sensing, Chromolaena odorata, WorldView-2, forest gaps, ROC*

[2] Malahlela, O.E., Cho, M.A., Mutanga, O., (in preparation). Integrating environmental and Worldview-2 data to map the probability of occurrence of *Chromolaena odorata* in forest gaps, Dukuduku coastal forest in KwaZulu-Natal, South Africa. *Biological Invasions Journal*

3.2 Introduction

Several alien plants are invading subtropical forest ecosystems through canopy gaps, resulting in the loss of native species biodiversity (Rand et al., 2004; Kolar and Lodge, 2001). The loss of native species in such habitats may result in reduced ecosystem functioning (Chapin et al., 2000; Whitmore, 1989; Macdonald et al., 1991). The control and eradication of these invaders requires accurate mapping of canopy gaps and modelling the extent of invasion in canopy gaps (Le Maitre et al., 1996; Underwood et al., 2003). Mapping the extent of invasive species may assist forest managers, conservation officers and all the relevant stakeholders to understand the extent of invasion and to allocate limited resources for the species eradication programmes (Reyers, 2004).

Commonly, identification of invasive species in forest gaps is done using ground-based surveys (Buckland et al., 1996; Scott et al., 2002). Using these methods, environmental data such as soil type, distance to trails/roads, distance to rivers, gap size and grass cover are collected and used for species prediction (Edwards et al., 2007). Although the collected environmental data is still useful in species prediction (Hirzel and Guisan, 2002), the success of using environmental data only is hampered by the amount of time and effort required to collect field data (Gu and Swihart, 2004; Margules and Pressey, 2000). Additionally, field surveys are inefficient in larger areas and less accessible terrain (Turner et al, 2003). To mitigate this problem, remote sensing technology is increasingly being employed as a rapid and cost-effective means for mapping the invasive species (Underwood et al., 2003; Joshi et al., 2006). Remote sensing data provides spatial vegetation cover over large geographical areas. This technology has been used for actual canopy cover mapping of invasive species dominating the canopy (Asner et al., 2008; Harding and Bate, 1991). In instances where the invasive species' spectral signatures do not dominate the canopy, the probabilistic mapping approach is adopted (Joshi et al., 2006; Laba et al., 2004).

Few studies have been conducted to map the probability of occurrence of non-canopy dominating invasive species using remote sensing and environmental data in indigenous forests. For example Joshi et al. (2006) used Landsat ETM + imagery together with environmental data to map the probability of occurrence of *Chromolaena odorata* in south central Nepal forest. However, remote sensing data such as Landsat, SPOT or IKONOS consist of spectral bands that tend to saturate in visible and near-infrared regions (Knipling, 1970; Mutanga and Skidmore, 2004). The development of new generation satellites such as

RapidEye (6.5 meters) and WorldView-2 (2 meters) has opened opportunities for improved savannah (Ramoelo et al., 2012) and forest vegetation (Mutanga et al., 2012; Ozdemir and Karnieli, 2012) biophysical characterization. The presence of new spectral bands in WorldView-2, such as the red edge band, has facilitated an improved characterization of vegetation structure and composition (e.g. greenness), than the common bands (Mutanga et al., 2012; Cho et al., 2012). This is due to the fact that the presence of these new bands (e.g. the red edge) solves the saturation problem that is common in common sensors, and therefore improves the prediction of chlorophyll, nitrogen and biomass (Ramoelo et al., 2012; Mutanga et al., 2012). In remote sensing, the "red edge" is the region of abrupt change in the leaf reflectance between 680 and 780 nm due to the combined effect of strong chlorophyll absorption in the red and high reflectance in the near-infrared wavelength resulting from the leaf's internal scattering (Horler et al., 1983). The question, therefore, is whether the new WorldView-2 bands such as red edge, can be related to the occurrence of invasive species in forest gaps? In addition, can the integration of ancillary environmental data (such as distance to roads, distance to rivers, DEM, gap size, gap perimeter and aspect) with new WorldView-2 spectral data improve the prediction of invasive species in forest gaps? Probability mapping of invasive species in vegetated gaps (gaps dominated by other species) is crucial for forest managers since it provides information on the likelihood of species occurrence before the invader could dominate the canopy (Pande et al., 2006).

Ancillary environmental variables (data) have been used to predict the distribution of species (Franklin, 1995) and their usage is still recognized continuously for species prediction, regardless of the limitation stated above (Yang et al, 2006; Václavík and Meentemeyer, 2009: Masocha and Skidmore, 2011). Therefore, the aim of the study is to integrate WorldView-2 data with ancillary environmental variables to map the probability of occurrence of invasive *Chromolaena odorata* (triffid weed) in forest gaps in the Dukuduku Coastal Forest of KwaZulu-Natal province, South Africa.

The objectives of the study are:

(a) To ascertain whether WorldView-2 bands are correlated with the distribution (presence or absence) of *Chromolaena odorata* in forest gaps.

(b) To determine whether the integration of WorldView-2 data with environmental data provides an improvement over the use of ancillary environmental data alone for predicting invasive species in forest gaps.

3.3 Methods

3.3.1 Study area

This study was undertaken in Dukuduku forest, located between the geographical co-ordinates of 28°38'33"S and 32°31'67" E, as part of the indigenous forest monitoring project of the Natural Resources and Environment at the South African Council for Scientific and Industrial Research (CSIR). The study area is located 11 km west of St. Lucia town on the northern coast of KwaZulu-Natal, South Africa (Fig. 9). It is one of the remaining coastal forests in the country that are threatened due to settlement expansion and invasion by exotic plant species. On the western side, the forest is surrounded by the sugar plantation farms and the *Eucalyptus* plantations, while on the eastern side there are villages that practise a different farming system, usually subsistence farming.

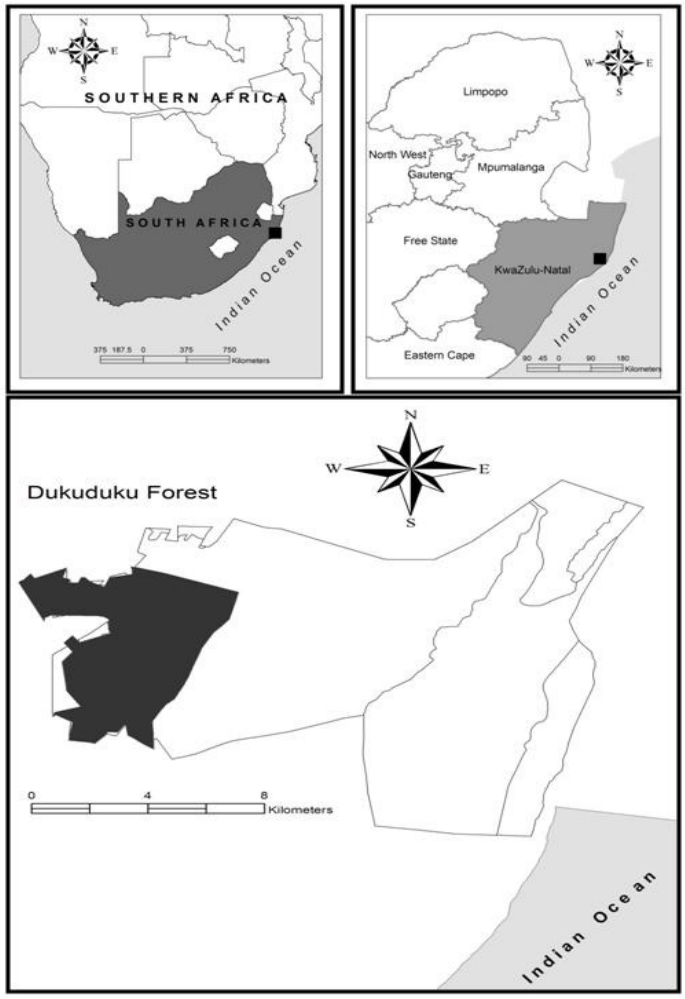

Fig.9 Map showing the location of the study area.

According to Van Wyk et al. (1996) the topography of the study area comprises of some minor north-south-trending dune ridges, which occur on a low plateau that rises to a maximum of 60m above the mean sea level. The soils in this area are mainly deep and predominantly derived from recent wind-deposited sands, with high leaching and poor nutrient status (Van Wyk et al., 1996).

The climate of KwaZulu Natal is subtropical, with high summer precipitations and high temperatures of over 33°C (between September and April). Winters are generally cooler (below 8°C), with the annual sea surface temperature of 15°C. The area receives annual rainfall of about 1 600 mm (Luwum, 2002).

3.3.2 Image acquisition and pre-processing

WorldView-2 imagery (acquired on 01 December 2010) with 8 spectral bands and at a 2 meter spatial resolution was used for the delineation of forest gaps. The imagery was geometrically corrected by the supplier, and the atmospheric correction was done using the AtCOR 2/3 software distributed by Rese Application. The atmospheric correction was based on the MODTRAN 5 module, which is a 'narrow band model' atmospheric radiative transfer code – with spectral range of between 0.2 to 100 µm (Berk et al, 1998). The atmospheric conditions specified in the ATCOR software for this image processing was the 'tropical rural' conditions.

3.3 .3 Field data collection

Field data was collected on two occasions and in different seasons with respect to logistical constraints. The first data collection was carried out in July 2011 (winter) while the second field data collection was carried out in October 2011 (late spring). The data collected included the location of forest gaps (using Vista eTrex ^{TM} GPS), as well as the presence or absence of invasive species (*Chromolaena*) in forest gaps. The collection of the data followed a line transect method. A simple random sampling technique was applied, where lines were randomly pre-selected to cover most parts of the forest. In total, 190 (n = 190) forest gaps were visited in the field. We used 2/3 (n = 114) of the data to construct a logistic regression model while 1/3 (n = 76) of data was used to validate the model.

3.3.4 Data analysis

The relationship between *Chromolaena odorata* presence or absence, environmental data and remote sensing data was modelled in logistic regression as shown in Fig. 10. A logistic regression was conducted for 3 sets of variables, i.e. (a) environmental variables only, (b) spectral variables only and (c) combined environmental and remote sensing variables in stepwise logistic regression.

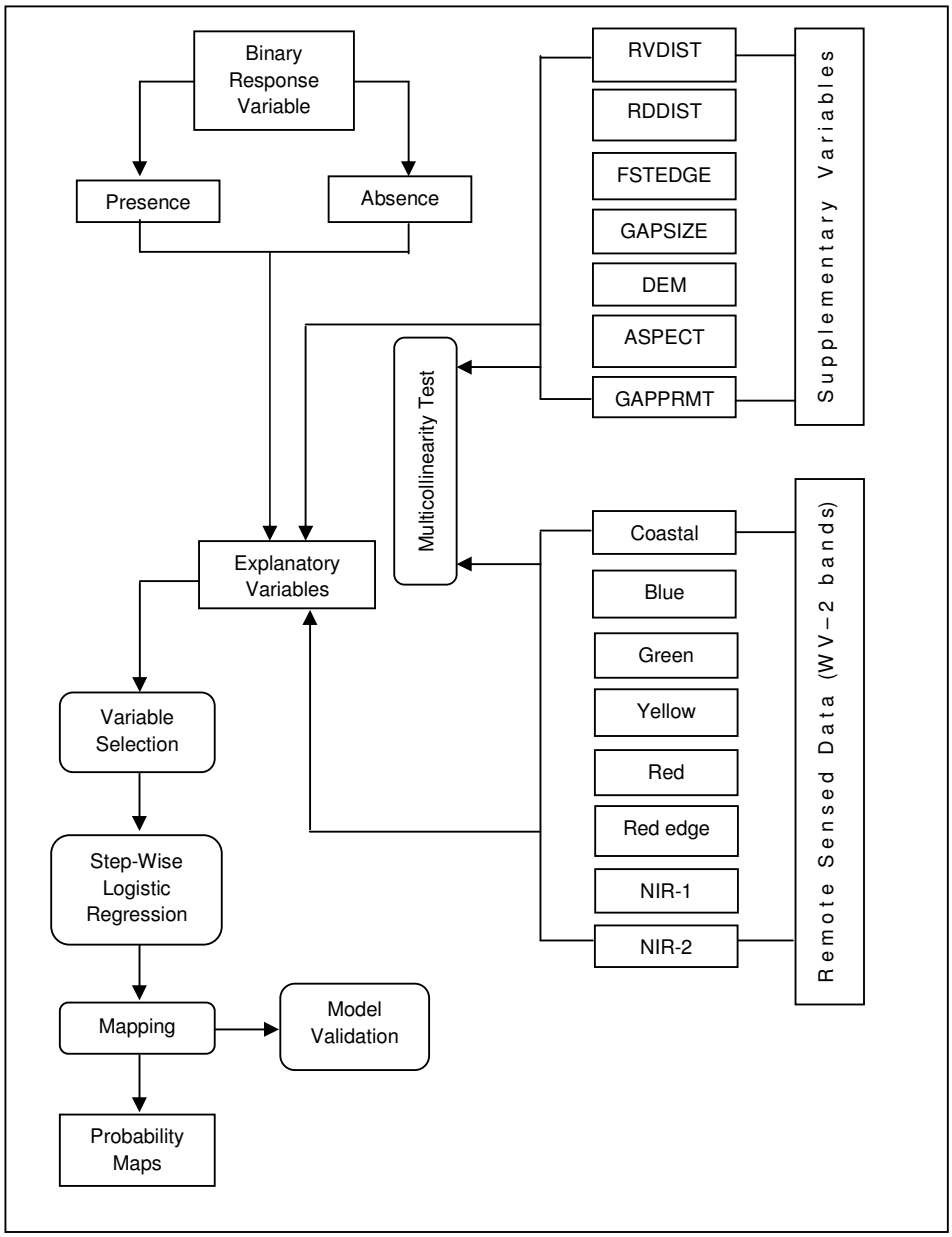

Fig. 10 Schematic representation of workflow followed during logistic regression modelling.

3.3.5 Ancillary environmental variables

Ancillary environmental data were used based on their availability and relevance to the aim and objectives of the study. The ancillary environmental dataset included digital elevation model (DEM) layer, aspect layer, distance to roads layer, distance to rivers layer, gap size layer, and gap perimeter layer.

a). DEM and Aspect

The digital elevation model (DEM) layer was generated from the 15 meter contour lines of the study area (Figure 11). Generation of the DEM is based on the algorithm ANUDEM, which calculates values on a regular grid of a discretised smooth surface fitted to a large number of irregularly spaced elevation data points, contour line data and stream line data (Hutchinson, 1996). Aspect layer was generated from a 15 meter DEM with the help of Spatial Analyst tool in ArcGIS software (Fig. 11 - right)

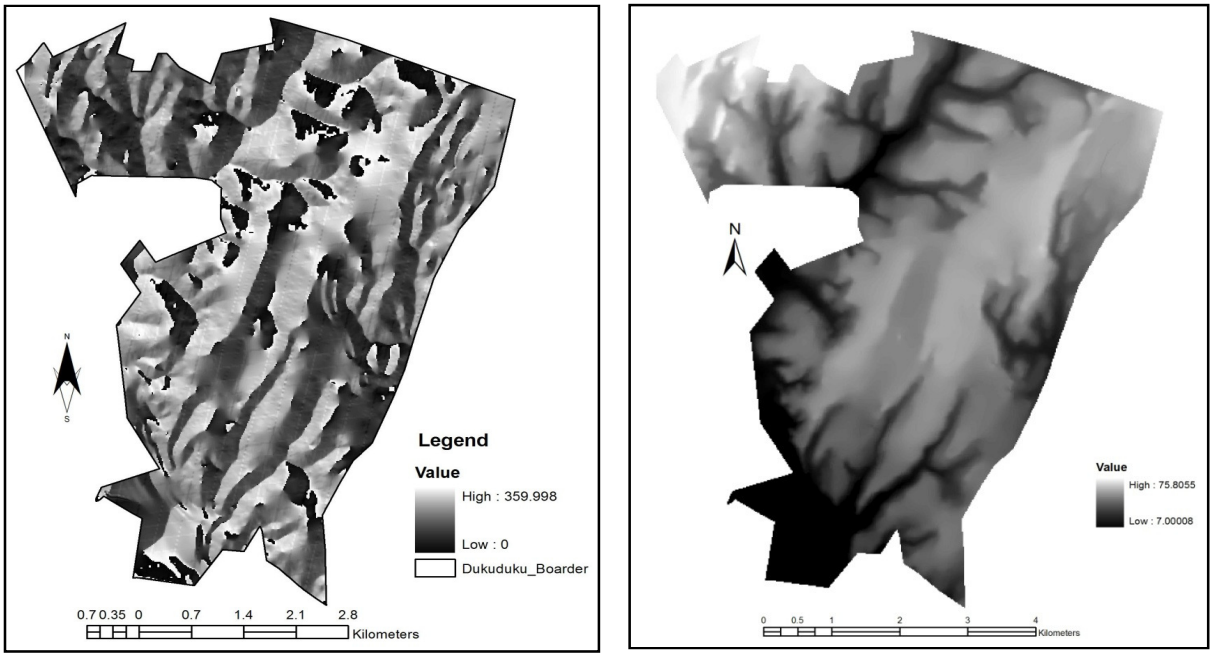

Fig. 11 Digital Elevation Model (left) and Aspect map derived from a 15 meter DEM (right)

b). Canopy gaps characteristics (size and perimeter)

Gap size and gap perimeter layers were generated from the WorldView-2 derived delineated forest canopy gaps (Fig. 12). Forest canopy gaps were delineated in object-based image analysis using the modified plants senescence index (Merzlyak et al., 1999). This technique yielded the highest accuracy of 93.69% when compared to pixel-based classification, and therefore the results were used to derive forest gap size and perimeter.

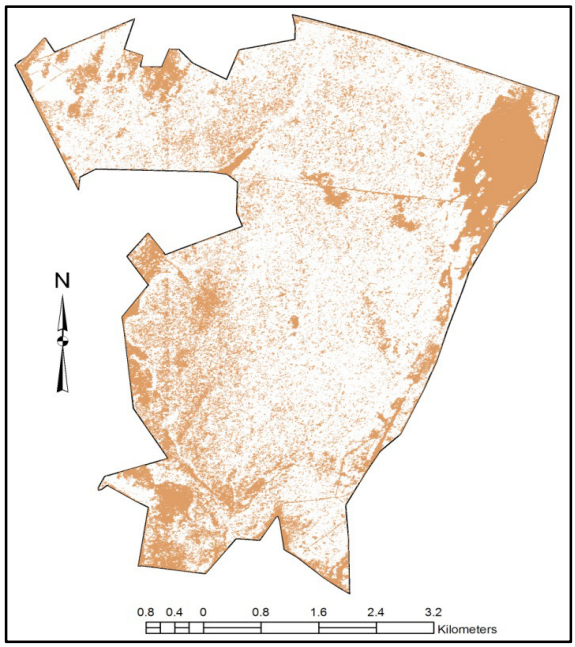

Fig. 12 Forest gap size and perimeter layer derived from delineated forest gaps map.

c). Distance to roads/paths

Distance to roads was generated from a road dataset in ArcGIS (Fig. 13 - left). The distances from roads were calculated from the forest gaps to the closest roads/paths. The forest's boundaries are mainly the main roads (national tar roads) and the gravel roads created for demarcating agricultural plantations.

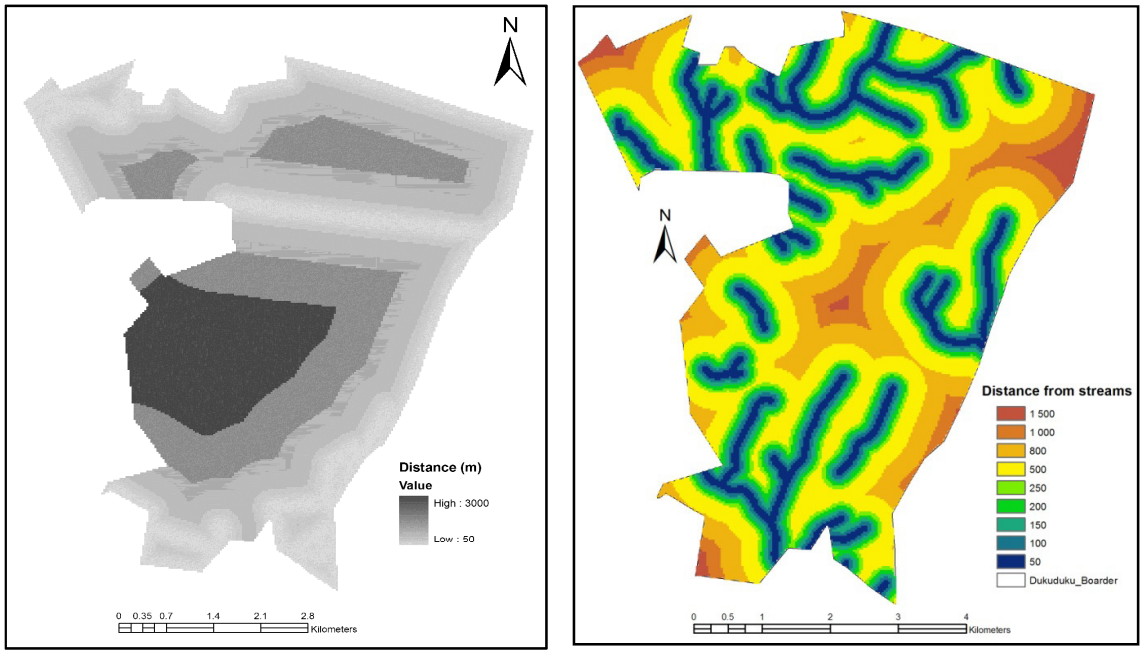

Fig. 13 The distance to roads map layer (left) and the distance to rivers (right) layer generated in ArcGIS.

d). Distance to rivers/streams

The distance to river map was derived from river and streams dataset of the study area. The generation of this map was done in ArcGIS (Fig. 13 - right). The distance was calculated from the forest gaps to the nearest rivers to determine the influence of rivers to the distribution of invasive species. The distances were measured in meters (m).

3.3.6 Spectral data

a). WorldView-2 bands

All eight (8) spectral bands of WorldView-2 bands (Fig. 14) were treated individually as separate input variables for prediction. These spectral bands have wavelength ranges of 400 – 450 nm (absorbed by chlorophyll), 450 – 510 nm (absorbed by chlorophyll), 510 – 580 nm (sensitive to plant health), 585 – 625 nm (absorbed by carotenoids – detects 'yellowness' of vegetation), 630 – 690 nm (absorbed by chlorophyll), 705 – 745 nm (sensitive to vegetation health), 770 – 895 nm (sensitive to leaf mass and moisture content) and 860 – 1040 nm (sensitive to leaf mass and moisture content) (Ustin et al., 2009).

b). Vegetation indices

Two sets of vegetation indices were tested for the regression. These sets are (i) indices that are commonly derived from common sensors, and (ii) indices that can be derived from WorldView-2 imagery. A total of seven (7) broadband and narrowband indices were tested for this study (Table 8).

Table 8
Vegetation indices used tested for invasive species prediction

Index	Formula	Application	Reference
$NDVI_{660}$	$NDVI = \frac{\rho_{830} - \rho_{660}}{\rho_{830} + \rho_{660}}$	Common index used to monitor vegetation vigour, health, vegetation cover and biomass. Values range from -1(bare surfaces) to 1(green plants).	Jackson et al.(1983)
SAVI	$SAVI = \left(\frac{\rho_{830} - \rho_{660}}{\rho_{830} + \rho_{660} + 0.5}\right) * (1 + 0.5)$	Common index used also for vegetation monitoring, biomass and vegetation health. It improves on NDVI by compensating for soil-background.	Huete (1988)
$NDVI_{725}$	$NDVI = \frac{\rho_{830} - \rho_{725}}{\rho_{830} + \rho_{725}}$	New WorldView-2 index that improves the detection of vegetation health, greenness, and biomass estimation. Values range from -1(bare surfaces) to 1(green vegetation).	Gitelson and Merzlyak (1994)
mPSRI	$mPSRI = \frac{\rho_{660} - \rho_{480}}{\rho_{725}}$	New WorldView-2 index used for detecting of leaf senescence, plant physiological stress and fruit ripening. Values range from -1(stressed canopy) to 1(less stressed canopy).	Merzlyak et al.(1999)
$NDVI_{545}$	$NDVI_{545} = \frac{\rho_{833} - \rho_{545}}{\rho_{833} + \rho_{545}}$	Common index that works similarly to $NDVI_{660}$ and additionally measures the greenness of vegetation	Gitelson et al.(1999)
EVI	$EVI = 2.5\left(\frac{\rho_{833} - \rho_{660}}{\rho_{833} + 6\rho_{660} - 7.5\rho_{480} + 1}\right)$	The enhanced vegetation index (EVI) is an 'optimized' index designed to enhance the vegetation signal with improved sensitivity in high biomass regions and improved vegetation monitoring through a de-coupling of the canopy background signal and a reduction in atmospheric influences.	Huete et al.(1997)
ARVI	$RVI = \frac{\rho_{833} - (2\rho_{660} - \rho_{480})}{\rho_{833} + (2\rho_{660} - \rho_{480})}$	An enhancement to the $NDVI_{660}$ that is relatively resistant to atmospheric factors (for example, aerosol). It uses the reflectance in blue to correct the red reflectance for atmospheric scattering. It is most useful in regions of high atmospheric aerosol content, including tropical regions contaminated by soot from slash-and-burn agriculture.	Kaufman and Tanre (1992)

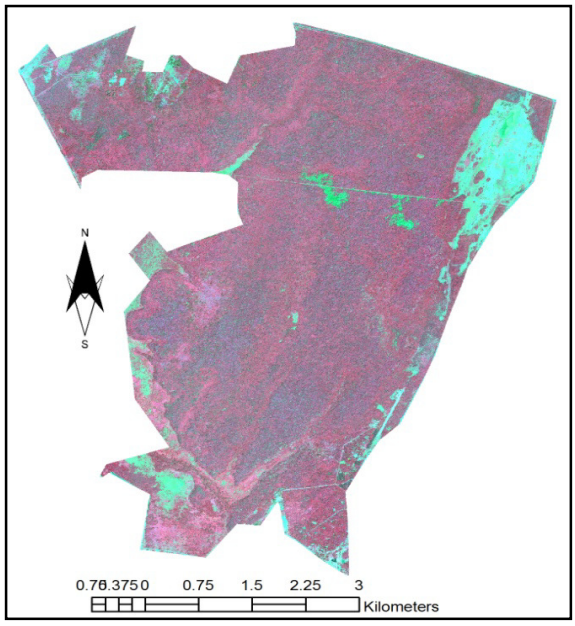

Fig. 14 A WorldView-2 imagery with 8 spectral bands

3.3.7 Model calibration

The dataset (n = 190) was randomly split into 2/3 (n = 114) for model calibration. The calibration dataset was used to train the model for invasive species occurrence using the R statistical software. A stepwise logistic regression was used for all input variables. In stepwise logistic regression, an attempt is made to eliminate any insignificant variable from the model before adding a significant one to the model and to deal with multicollinear variables. The choice of the model was dictated by the binary nature of the response variable (presence or absence), its simplicity for embedding in a GIS software (Yang et al, 2006) and its popularity amongst all other predictive models (Manel et al., 1999; Aspinall, 2002). Logistic regression is given by the following equation:

$$\rho = \left(\frac{e^{\beta_0 + \beta_1 x_1 + \beta_2 x_2 \ldots \beta_n x_n}}{1 + e^{\beta_0 + \beta_1 x_1 + \beta_2 x_2 \ldots \beta_n x_n}}\right) \qquad \text{Eq: 1}$$

where ρ is the probability of occurrence, x_n is the explanatory variable, b_n is the coefficient of x_n, β_0 is the intercept and e is the exponent function of the model. The final model goodness

of fit was measured by the deviance (D^2) which is an analogy to a coefficient of determination (R^2) (Rossiter and Loza, 2010). The D^2 is obtained from the following equation:

$$D^2 = 1 - \left(\frac{residual\ deviance}{null\ deviance}\right) \quad \text{Eq: 2}$$

Each removal or addition from or to a model is listed as a separate step in the model output. The model with the highest D^2 and lowest Aikaike's Information Criterion (AIC) was selected as the most ideal model because it has the best fit (Fox, 2002).

3.3.8 Model validation

One-thirds of the data (n = 76) was used for validating the predictive model. The predicted probabilities (y), which ranged from values between 0 and 1, represented the increasing probability of *Chromolaena* presence in forest gaps. A range of thresholds was explored to determine the optimum threshold level for predicting *Chromolaena* presence and absence (P/A) in forest gaps. The study by Manel et al. (1999) previously suggested a probability threshold value of 0.5 as the optimum threshold value for species prediction, although this value may not be ideal in all cases. For this study, we tested probability thresholds of 0.2 – 0.9 as shown in table 10. A 2x2 error matrix table (with rows indicating predicted cases and columns indicating observed cases) was plotted for a threshold value that yielded the highest mapping accuracy. The overall mapping accuracy is defined as the total number of the correctly predicted test cases to the total number of test samples, and is presented as a percentage (Fielding and Bell, 1997). The table compares the predicted values (from an optimum threshold value) with the observed field data of *Chromolaena* distribution.

The area under the ROC (AUC) has been used in several studies in order to understand the robustness of the model for a binary classifier (Egan, 1975; Swets et al., 2000; Fawcett, 2006). The AUC value of 0.5 indicates that the model accuracy is equal to the random prediction, while the value of 1.0 shows the perfect model fit (Baldwin, 2009). In essence, the AUC has a quantitative measure on a 0.0 to 1.0 scale, with the following grading levels:

- < 0.6 indicates a poor model

- 0.6 – 0.7 indicates a pass model
- 0.7 – 0.8 indicates a good model
- >0.9 indicates an excellent model

Furthermore, the sensitivity and specificity analysis was performed across the probability range from 0.2 – 0.9. For binary error matrix, sensitivity is defined as the proportion of correctly classified presence to the total number of presences in the test samples. On the other hand, specificity is the proportion of correctly predicted absence to the total number of absence in test samples (Fielding and Bell, 1997).

3.4 Results

3.4.1 Logistic regression

The combined environmental and spectral data model yielded the highest mapping accuracy, with the D^2 of 0.42. The D^2 of 0.42 indicates that the model can explain about 42% of the variability of presence or absence data of *Chromolaena odorata*. From this model, two of the environmental variables (distance to rivers and aspect) were significant at *alpha* < 0.05.

Table 9
Selected significant models resulting from the stepwise from logistic regression analysis (shown by *)

Data Source	Predictor	Estimate	Std. Error	*z* value	*ρ* value
Environmental Variables (D^2 = 0.12)	(Intercept)	1.2299	0.9033	1.362	0.1733
	Distance to Rivers	0.00238	0.0014	1.998	0.0457 *
	Distance to Roads	0.0015	0.0014	1.057	0.2906
	DEM	- 0.0020	0.0039	- 0.511	0.6096
	Aspect	0.0019	0.0037	0.499	0.6176
	Gap Size	- 0.0019	0.0025	- 0.773	0.4395
WorldView-2 Variables (D^2 = 0.20)	(Intercept)	- 0.4237	9.2840	- 0.046	0.9639
	Coastal Band	0.0497	0.0340	1.459	0.1446
	Blue Band	- 0.0005	0.0159	- 0.033	0.9738
	Green Band	0.0345	0.0647	0.533	0.5942
	Yellow Band	- 0.0186	0.0250	- 0.742	0.4583
	Red Band	- 0.0840	0.0953	- 0.882	0.3777
	Red Edge Band	- 0.0703	0.1734	- 0.405	0.6854
	Near Infrared-1	0.1596	0.1362	1.172	0.2413
	Near Infrared-2	- 0.0557	0.0315	- 1.769	0.0769
	SAVI	12.7000	10.5400	1.205	0.2284
	MPSRI	- 0.0613	0.00755	- 0.812	0.4169
	$NDVI_{660}$	- 12.6700	10.5700	- 1.199	0.2307
	$NDVI_{725}$	- 28.0700	16.3200	- 1.720	0.0085 **
	ARVI	0.1965	0.1288	1.526	0.1270
	$NDVI_{545}$	- 0.1554	0.1051	- 1.478	0.1394
	EVI	- 0.0122	0.0101	- 1.202	0.2294
Combined Model (D^2 = 0.42)	(Intercept)	2.4447	7.8896	0.310	0.7567
	Distance to Rivers	0.0064	0.0028	2.255	0.0241 *
	Aspect	0.0121	0.0057	2.105	0.0353 *
	Distance to Roads	0.0036	0.0026	1.363	0.1727
	Gap Perimeter	- 0.0072	0.0067	- 1.082	0.2794
	Coastal Band	0.0830	0.0418	1.988	0.0468 *
	Yellow Band	- 0.0389	0.01735	- 2.243	0.0249 *
	Red Band	0.1264	0.0914	1.353	0.1760
	Near Infrared-1	0.3140	0.1487	2.112	0.0347 *
	Near Infrared-2	- 0.1032	0.0481	- 2.146	0.0319 *
	$NDVI_{545}$	- 0.2164	0.1155	- 1.875	0.0608
	SAVI	22.5007	14.8667	1.514	0.1302
	mPSRI	- 0.1741	0.1127	- 1.545	0.1222
	$NDVI_{660}$	- 22.3567	14.8628	- 1.504	0.1325
	$NDVI_{725}$	- 49.8962	25.3571	- 1.968	0.0491 *
	ARVI	0.0235	0.1215	1.921	0.0547

Significance codes: ***(*), 0.05*** ***(**), 0.01*** ***(***), 0,001***

Also, from this model, five (5) of the spectral data variables (coastal band, yellow band, near-infrared1, near-infrared2 and $NDVI_{725}$) were the most significant at *alpha* < 0.05. About 60% of the significant spectral variables (3 out of 5) showed a negative relationship with the presence or absence of *Chromolaena*. The yellow band (λ_{605} nm), the NIR-2 band (λ_{950} nm), and the red edge NDVI ($NDVI_{725}$) showed a significant negative relationship to *Chromolaena* presence or absence in forest gaps. On the other hand, the coastal (λ_{425} nm) and near-infrared1 (λ_{833} nm) bands showed a positive relationship to the occurrence of *Chromolaena* (Table 9).

The results show that WorldView-2 data alone explained about 20% (D^2 = 0.20) of the variability of invasive *Chromolaena* presence or absence in forest gaps. Among the WorldView-2 only data, the $NDVI_{725}$ was the only significant variable at *alpha* < 0.05. Among the environmental data only, the distance to rivers was the most significant positive variable at *alpha* < 0.05. Figure 15 shows the predicted probability of occurrence of invasive species across the delineated forest gaps. High probabilities of *Chromolaena* presence are shown by brown colour, while low probabilities are shown by yellow colour.

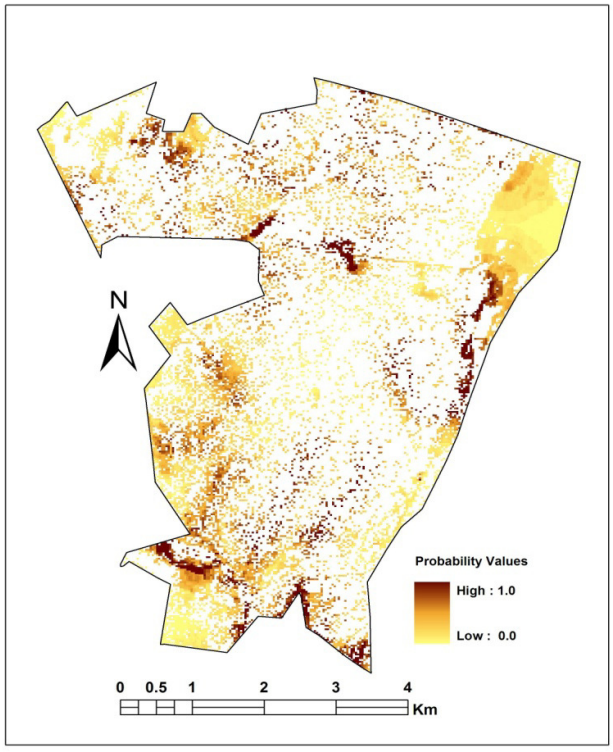

Fig. 15 Probability map of *Chromolaena odorata* in forest gaps.

3.4.2 Model validation

The predictive model (binary outcome value range of 0.0 – 1.0) was validated using probability threshold values as shown in table 10. The highest mapping accuracies were obtained at thresholds of 0.3 and 0.5 (both at 86.8%). The highest sensitivity rates were observed at threshold values of 0.2 and 0.3 (91.0%). The highest specificity rates were obtained at the threshold values of 0.7, 0.8 and 0.9 (all at 88.8%). The 2x2 error matrix table for a probability threshold of 0.5 is shown in table 11.

Table 10
Statistics for evaluating model performance across threshold values

	Threshold values							
	0.2	**0.3**	**0.4**	**0.5**	**0.6**	**0.7**	**0.8**	**0.9**
Mapping accuracy (%)	85.5	86.8	85.5	86.8	85.5	82.8	81.5	75.0
Sensitivity (%)	91.0	91.0	89.5	88.0	86.5	82.0	80.6	73.1
Specificity (%)	44.4	55.5	55.5	77.7	77.7	88.8	88.8	88.8

Table 11

Predicted outcomes (y) from logistic regression on *C. odorata* vs. the observed field data at probability threshold of 0.5 ($\rho = 0.5$)

Observed	***Predicted***		***Total***
	Presence	Absence	
Presence	59	8	67
Absence	2	7	9
Total	61	15	76

The robustness of the model (curve) was also measured by the Area Under the Curve of receiver operating characteristic (ROC) curve (Fig. 16). The validation dataset yielded an AUC of 0.9187 (*good* model). The diagonal line in the model represents the strategy of randomly guessing a class (Fawcett, 2006). If the curve bends towards or below the diagonal line (decreasing sensitivity) this indicates a poor model. A good model is the one whose curve bends towards the north-western direction of the plot (Fawcett, 2006). Our ROC shows that our curve bends towards the north-western direction, and hence an AUC of 0.9187.

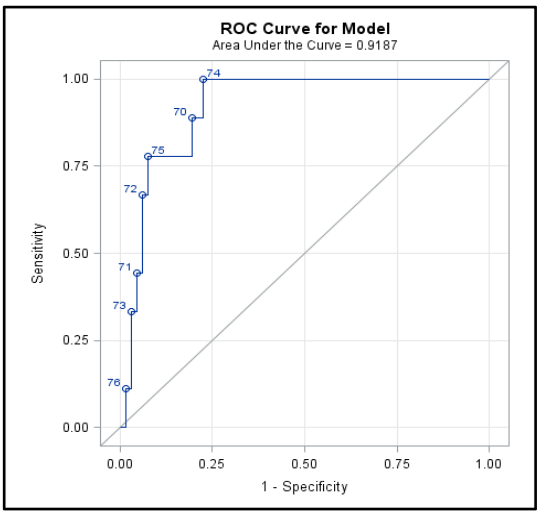

Fig. 16 ROC curve generated from the independent validation dataset

3.5 Discussion

The findings of the study suggest that there is a relationship between WorldView-2 spectral bands and the presence or absence of invasive *Chromolaena odorata* (Table 9). The model that combined the environmental variables and spectral variables yielded a high prediction accuracy, which underscores the importance of such variables in the prediction of *C. odorata* in forest gaps. This combination is necessary since on their own, the ancillary environmental variables or WorldView-2 data do not yield mapping accuracies greater than 20%. The general trend depicted by the predictive model shows that the probability of occurrence of *C. odorata* tend to increase in forest gaps that are less vegetated than those that are densely vegetated. This trend is supported by observing the predictive model's spectral estimates of the coastal band (λ_{425} nm), yellow band (λ_{605} nm), the NIR-2 (λ_{950}nm) and the red edge NDVI ($NDVI_{725}$), which are significantly correlated with the presence and absence data of *C. odorata*. A negative estimate of $NDVI_{725}$ means that the presence of *C. odorata* decreases with increasing density of vegetation, as an increase in $NDVI_{725}$ is associated with increases in vegetation densities or biomass. Similar findings were achieved by Joshi et al. (2006) who observed that *C. odorata* does not thrive in densely vegetated forest areas. These findings show that the red edge (used to compute $NDVI_{725}$) is significant in mapping the probability of occurrence of *C.odorata*, which is in line with the assumption made for this study, as set out in chapter 1. The increase in reflectance in the NIR-1 region may be associated with the fact that sampled forest gaps not only comprised of vegetation, but also of bare soil, logs and plant litter that may have influence on the spectral behavior in this region – a phenomenon that require further investigation.

The environmental variables such as distance to rivers and streams and aspect proved to be positively significant in determining the presence and absence of occurrence of *C. odorata*. The implication is that as one advance closer to the streams, the probability of finding *C. odorata* increase, and this is in line with the findings by Joshi et al. (2006) and Van Gils et al., (2006) who found areas closer to roads to be more likely invaded by *C. odorata*. The results also showed that the probability of invasive species occurrence increases with the orientation of aspect towards the north. This implies that one is more likely to find invasive species in north facing slopes, than the south facing slopes. This is due to the fact that north-facing slopes in the southern hemisphere are warmer than south-facing slopes (Adams, 2010). The species triumphs in areas that are open, with appropriate light and temperature ranges of between 20 - 37˚C, and hence the increase in slope direction (towards the north) increases

probability of finding *C. odorata* (Gareeb, 2007). Invasive *C. odorata* also prefers forest gaps that are closer to the streams due to their competitive nature for water and essential mineral resources. This trend is in line with the findings by Goodall and Zacharias (2002) who observed that this invasive species prefers forest margins and is often found along rivers or streams. On the whole, the pattern of the probability of occurrence (figure 15) indicate that *Chromolaena* is less likely to occur in pristine forest than in the areas that are open, such as closer to the roads or at the edges of forest.

3.5.1 Management of invasive species

The management of invasive species such as *C. odorata* has been debated in different countries, globally. For example Herren-Gemill (1991) described the need to control *Chromolaena odorata* due to its high frequency of occurrence in invaded fallow sites in West Africa. From the conservation point of view, management and control priority should be focused on the species' habitat and future distribution of species (Rowe, 1992), and not solely on the degradation levels caused by this species (Goodall and Erasmus, 1996). Mapping the probability of occurrence of invasive species in its potential habitats (forest gaps) is crucial to the management geared towards eliminating such species.

Fig. 17 Myself (Oupa) showing a probability map to the forest weed eradication workers at the Dukuduku coastal forest. Workers are seen with eradication tools and chemical spray tanks applied at the stumps of controlled species.

The output maps serve as a guideline to fieldworkers and forest managers for the identification of probable habitats of *C. odorata* and for man-power recruitment.

In South Africa, for example, there are projects that are aimed at eradicating invasive *C. odorata* in the coastal forests, such as the Dukuduku forest (Fig.17), where field workers were assigned to walk randomly through the forest to eradicate visible invasive species. The modeling of invasive species probability of occurrence could potentially assist in eliminating the random search of invasive species by providing key indications of areas of high probability of occurrence.

3.6 Conclusion

In conclusion several key points were found for the study:

- The WorldView-2 bands are correlated with the presence or absence of invasive *Chromolaena odorata* in forest gaps.
- The coastal blue (λ_{425} nm), NIR-1 (λ_{833} nm), yellow (λ_{605} nm), NIR-2 (λ_{950} nm) and red edge NDVI bands ($NDVI_{725}$) are significantly related to the occurrence of invasive species in forest gaps. The probability of finding *Chromolaena* increases with decreasing reflectance in the regions of electromagnetic spectrum of yellow, NIR-2 regions and the red edge NDVI. This implies that one is more likely to find *Chromolaena* in forest gaps that are not densely vegetated. The relationship of the probability of occurrence with the coastal band also supports this observation.
- The environmental data-only model explained the variability of about 12% of invasive *Chromolaena* presence or absence in forest gaps.
- The final combined model of WorldView-2 spectral data and ancillary environmental data increased predictive model accuracy to 42% (D^2 = *0.42;* WorldView-2 data added) from 12 % (D^2 = *0.12;* environmental data only), which emphasizes the advantage of integrating WorldView-2 with the ancillary environmental data for invasive species mapping.

Chapter Four

Conclusions and Recommendations

4.1 Introduction

Mapping the probability of occurrence of invasive plant species has been of special interest to researchers, planners, federal governments, ecologists and park managers over the years (Laba et al., 2004; Jarošik et al., 2011; Le Maitre, 2002; Joshi et al., 2006). Appropriate data and analytical techniques can improve the detection of invasive species habitats and establish the relationship between the species' presence or absence and the conditions that promote the establishment of such species. A combination of remote sensing data and field data proved to be crucial in mapping the occurrence of invasive species in this study, although this was previously done on a very coarse resolution scale (Rew et al., 2005; Joshi et al., 2006; Masocha and Skidmore, 2011). This study showed that the improvement in remote sensing imagery resolution (spatial and spectral) could potentially be imperative in detecting invasive species habitats, and that integrating spectral data with environmental variables could improve the mapping accuracy of *Chromolaena odorata* 's probability of occurrence. The main aim of this study was to test the potential of integrating high resolution WorldView-2 data with ancillary environmental data to map the probability of occurrence of invasive *Chromolaena odorata* in the forest gaps of Dukuduku coastal forest. The main objectives were, therefore: (i) to explore the utility of WorldView-2 multispectral bands for delineating forest canopy gaps, (ii) to investigate the performance of an object-based classification technique and pixel-based classification methods for delineating forest canopy gaps, and (iii) to test whether the integration of WorldView-2 imagery with ancillary environmental data can improve the modeling of *Chromolaena odorata* presence and absence in forest gaps using a logistic regression model.

4.2 Exploring the utility of WorlView-2 multispectral bands for delineating forest canopy gaps

Delineating forest gaps using an 8 band WorldView-2 image was confirmed by the findings in this study. The maximum likelihood classifier applied on a spectrally resampled 4-band image, common in SPOT, IKONOS and Landsat imagery, showed a drop in average user and overall classification accuracies (from 86.33% to 70.83%, and from 86.90% to 74.64%

respectively), which is an indication that new WorldView-2 band provide spectral enhancement to the common RGB and NIR bands (Mutanga et al., 2012; Cho et al., 2012; Ozdemir and Karnieli, 2011). This highlights that WorldView-2 bands can improve on the discrimination of forest gaps from other forest classes by minimizing the spectral saturation problem common in common sensors (Cho et al., 2008, Mutanga et al., 2012). The pixel-based overall classification accuracy resulting from WorldView-2 bands is 15.50% higher than overall classification accuracy derived from common RGB and NIR bands. This finding highlights the significance of WorldView-2 bands for improved forest vegetation class discrimination.

4.3 Investigating the performance of an object-based classification technique and pixel-based classification methods for delineating forest canopy gaps

Pixel-based classification has been used for ecological applications and in other fields of study (Couturier et al., 2009; Wulder et al., 2003; Albert, 2002). However, the use of pixel-based classification results in a 'salt-and-pepper' effect which can be a problem for forest gap delineation. In order to overcome this problem, this study successfully employed the use of object-based classification using vegetation indices as a proxy. Object-based image classification has an advantage over pixel-based classification in that it groups together the pixels of particular similarity as defined by particular homogeneity criteria. This generalization resulted in the possibility of extracting forest gaps, which sets the baseline for probability analysis at a later stage (i.e. derivation of forest gap size layer). By comparison, the accuracy assessment of classifiers revealed that object-based classification using vegetation indices (mPSRI) outperformed common classification method (MLC), with the user accuracy of 90.26% and 86.14% respectively. The results from McNemar's test showed that there is a statistical difference between the classification results obtained from the pixel-based MLC analysis, and those obtained from the mPSRI object-based analysis. The mPSRI object-based analysis yielded the highest average producer accuracy (92.18%) in comparison to the MLC technique, which yielded the average producer accuracy of 86.33% for all forest classes. Further integration of these methods together with post-classification refinement may result in improved classification accuracies for the delineation of forest canopy gaps.

4.4 Test of whether the integration of spectral data with supplementary data can improve the probability of occurrence of Chromolaena odorata in forest gaps

The model derived from a combination of WorldView-2 and environmental data yielded the highest D^2 of 0.42 compared to the environmental data-only model and to the WorldView-2 data-only model. This means that about 42% of the variability of *Chromolaena odorata* presence or absence can be explained by this model. The findings from this study showed that as the distance to roads increases, and as the slope orientation is inclined towards the north, the probability of finding *C. odorata* in forest gaps increases. WorldView-2's coastal band, yellow band, NIR-2 and the red edge NDVI provided a clear indication of the conditions within the forest gaps which increase the probability of occurrence of *C. odorata*. The combined model indicates that as the light reflectance in the coastal band increases, and the light absorption increases in the yellow and NIR-2, then the probability of occurrence of *Chromolaena* also increase. On its own the model generated from environmental data only showed a D^2 of 0.12, while the model generated from spectral data only yielded a D^2 of 0.20.

4.5 Conclusions

The aim of this study was to investigate the potential of WorldView-2 in mapping the probability of occurrence of *C. odorata* in subtropical forest canopy gaps. This study has shown that it is possible to map the occurrence of invasive *C. odorata* in forest gaps using a combined model of environmental variables and WorldView-2 variables derived from a logistic regression. In line with the aim and objectives of the study the following concluding remarks were drawn from the findings:

1. WorldView-2 image improved the delineation of forest canopy gaps, by yielding the overall classification accuracy of 86.90% which was higher than the common red, green, blue and NIR bands (common in SPOT and Landsat), which yielded overall classification accuracy of 74.64%.

2. The modified plant senescence index (mPSRI) in object-based image analysis yielded the highest overall accuracy (93.69%) than the pixel-based maximum likelihood classifier (86.90%). The mPSRI is an index that utilizes the reflectance in the red edge band, which is a new band to the WorldView sensor. The reduction of the "salt-and-pepper" effect in object-based classification improves the discrimination of forest vegetation classes, than the pixel-based classification. However, maximum likelihood classifier still offers reliable classification accuracies in the category of pixel-based classifiers.

3. WorldView-2 imagery data improves the predictive model accuracy of invasive species when integrated with additional environmental data. The model used to predict the occurrence of *C.a odorata* in forest gaps yielded a D^2 of 0.42, meaning that the model can explain about 42% of the variability in the presence and absence of this alien plant in forest gaps. This D^2 is the highest, compared to the environmental data only model ($D^2 = 0.12$) and WorldView-2 data only model ($D^2 = 0.20$).

4.6 Recommendations

1 WorldView-2 imagery has shown to have the capability to delineate forest gaps in the study area. Vegetation indices utilizing WorldView-2 red edge band (centred at λ_{725} nm) yielded increased classification accuracies for discriminating the four classes of forest vegetation and thus making it possible to delineate forest gaps(both vegetated and non-vegetated gaps). The vegetation indices utilizing the yellow band (λ_{605} nm) and the coastal band (λ_{425} nm) yielded poor classification accuracies. It is therefore, recommended that vegetation indices that can employ the use of these bands be explored to increase their sensitivity to detect change in vegetation classes.

2 The study has shown that the environmental variables are important for mapping the probability of occurrence of invasive species, although the variables used yielded lower D^2 of 0.12. However, the addition of variables such as grass cover, soil type, gap connectivity, species age and seed production could potentially increase prediction accuracy of the model. It is also recommend that size of the collected field

data be expanded to capture varying conditions under which invasive species may occur.

3 Previous studies have indicated that mapping the invasive species occurrence forms part of the crucial management guidance for species eradication. For example, Hirzel and Giusan (2002) have pointed out that the sampling strategy can increase the probability of finding an invasive species when the occurrence of the invader is known to be correlated with a particular variable(s). Future research should focus on establishing additional environmental factors that favour the invasive *C. odorata* distribution as well as a sampling strategy that increases the probability of finding *C.odorata* at an early stage.

References

Adair, R.J., Groves, R.H., 1998. Impacts of Environmental Weeds on Biodiversity: A Review and Development of a Methodology. Biodiversity Group, Environment Australia, Canberra.

Adams, J., 2010. Vegetation – Climate Interaction. "How Plants Make the Global Environment". Second Edition, Springer. ISBN 978-3-642-00880-1.

Adams, M. L., Philpot, W. D., Norvell, W. A., 1999. Yellowness index: An application of spectral second derivatives to estimate chlorosis of leaves in stressed vegetation. *International Journal of Remote Sensing 20***,** 3663-3675.

Albert, T.H., 2002. Evaluation of remote sensing techniques for ice-area classification applied to the tropical Quelccaya ice-cap, Peru. *Polar Geography* 26, 210-226.

Andrew, M.E., Ustin, L.E., 2008. The role of environmental context in mapping invasive plants using hyperspectral image data. *Remote Sensing of Environment* 112, 4301–4317.

Anon, 1997. Malaysian loggers in the Amazon. Action Alert, Rainforest Action Network, 24 February 1997.

Asner, G. P., Heidebrecht, K. B., 2002. Spectral unmixing of vegetation, soil and dry carbon cover in arid regions: comparing multispectral and hyperspectral observations. *International Journal of Remote Sensing* 23, 3939–3958.

Asner, G. P., Keller, M, Pereira, R., Zweede, J. C. Silva, J. N. M., 2004. Canopy damage and recovery after selective logging in Amazonia: field and satellite studies *Ecological Applications* 14, S280–98.

Aspinall, R., 2002. The use of logistic regression for validation of maps of the spatial distribution of vegetation species derived from high spatial resolution hyperspectral remotely sensed data. *Ecological Modeling* 157, 301-312.

Baatz, M., Bentz, U., Dehghani, S., Heynen, M., 2004. eCognition User Guide 4. Definiens Imaging, Műnchen.

Baldwin, R.A., 2009. Use of Maximum Entropy Modelling in Wildlife Research. *Entropy* 11, 854-866.

Battles, J.J., Dushoff, J.G., Fahey, T.J., 1996. Line intersects sampling of forest canopy gaps. *Journal of Forest Science* 42, 131-138.

Bauer, M.E. et al., 1986. Field Spectroscopy of Agricultural Crops. *IEEE Transactions on Geoscience and Remote Sensing* GE-24, 65-67.

Berk, A., Bernstein, L., Anderson, G., Acharya, P., Robertson, D., Chetwynd, J., & Adler-Golden, S., 1998. MODTRAN cloud and multiple scattering upgrade with application to AVIRIS. *Remote Sensing of Environment* 65, 367– 375.

Betts, H.D., Brown, L.J., Stewart, G.H., 2005. Forest canopy gap detection and characterization by the use of high-resolution Digital Elevation Models. *The New Zealand Journal of Ecology* 29, 95–103.

Blackburn, G.A., Milton, E.J., 1996. Filling the gaps: remote sensing meets woodland ecology: *Global Ecological Biogeography Letters* 5, 175-191.

Blaschke, T., 2010. Object based image analysis for remote sensing. *ISPRS Journal of Photogrammetry and Remote Sensing* 65, 2-16.

Blaschke, T., Strobl, J., 2001. Whats wrong with pixels? Some recent developments interfacing remote sensing and GIS. *GeoBIT/GIS* 14, 12–17.

Boon, R., 2010. *Pooley's trees of eastern South Africa: A complete guide*. Flora and Fauna Publications Trust. 2nd Edition.

Borak, J.S., Strachler, A.H., 1999. Feature selection and land cover classification of a MODIS-like data set for a semi-arid environment. *International Journal of Remote Sensing* 20, 919-938.

Bork, E.W., Su, J.G., 2007. Integrating LiDAR data and multispectral imagery for enhanced classification of rangeland vegetation: A meta analysis. *Remote Sensing of Environment* 111, 11-24.

Bradshaw, G.A., Spies, T.A., 1992. Characterizing canopy gap structure in forests using wavelet analysis. *Journal of Ecology* 80, 205-215.

Brokaw, N., Grear, J., 1991. Forest structure before and after hurricane Hugo at three elevations in Liquillo Mountains, Puerto Rico. *Biotropica* 23, 386-392.

Brokaw, N.V.L., 1982. The definition of tree fall gap and its effect on measure of forest dynamics. *Biotropica* 11, 158-160.

Brokaw, N.V.L., 1985. Gap-phase regeneration in a tropical forest. *Ecology* 66, 682-687.

Buckland, S.T., Elston, D.A., Beaney, S.J., 1996. Predicting distributional change, with application to bird distributions in northeast Scotland. *Global Ecology and Biogeography Letters* 5, 66–84.

Chapin III FS, Zavaleta ES, Eviner VT et al. (2000) Insight on Consequences of Changing Biodiversity. *Nature* 405, 234-242 .

Chen, Q., 2009. Improvement of the Edge-based Morphological (EM) method for lidar data filtering. *International Journal of Remote Sensing* 30, 1069-1074.

Cho, M.A., Mathieu, R., Asner, G.P., Naidoo, L., Van Aardt, J., Ramoelo, A., Debba, P., Wessels, K., Main, R., Smit, I.P., Erasmus, B., 2012. Mapping tree species composition in South African savannas using an integrated airborne spectral and LiDAR system. *Remote Sensing of Environment* 125, 514-226.

Cho, M.A., Skidmore, A.K., Atzberger, C., 2008. Towards red-edge positions less sensitive to canopy biophysical parameters for leaf chlorophyll estimation using properties optique spectrales des feuilles (PROSPECT) and scattering by arbitrarily inclined leaves (SAILH) simulated data. *International Journal of Remote Sensing* 29, 2241-2255.

Clark, D.B., 1990. The role of disturbance in the regeneration Neotropical moist forests. In K. S. Bawa, and M. Hadley (Eds.). Reproductive Ecology of Tropical Forest Plants, pp. 291–315, UNESCO & Parthenon, Paris, France.

Clark, M. L., Clark, D.B., Roberts, D.A., 2004. Small-footprint lidar estimation of sub-canopy elevation and tree height in a tropical rain forest landscape. *Remote Sensing of Environment* 91,68–89.

Congalton, R.G. 1991. A review of assessing the accuracy of classifications of remotely sensed data. *Remote Sensing of Environment* 37, 35-46.

Couturier, S., Gastellu-Etchegorry, J.P., Patiñ, P., Martin, E., 2009. A model-based performance test for forest classifiers on remote-sensing imagery. *Forest Ecology and Management* 257, 23–37

Cronk, Q., Fuller, J., 1995. Plant Invaders. The Threat to Natural Ecosystems. Chapman and Hall, London.

Davis, M.A, Grime, P.J., Thompson, K., 2000. Fluctuating resources in plant communities: a general theory of invasibility. *Journal of Ecology* 88, 528-534.

Dean, A.M., Smith, G.M., 2003. An evaluation of per-parcel and land cover mapping using maximum likelihood class probabilities, *International Journal of Remote Sensing.* 24, 2905-2920.

Denslow, J.S., 1987. Tropical rainforest gaps and tree species-diversity. *Annual Review of Ecology and Systematics* 18, 431-451.

Digital Globe, 2009. The benefits of 8 spectral bands of WorldView-2. White paper. www.digitalglobe.com.

Duveiller, G., Defourny, P., Desclee, B., Mayaux, P., 2008. Deforestation in Central Africa: Estimates at regional, national and landscape levels by advanced processing of systematically-distributed Landsat extracts. *Remote Sensing of Environment* 112, 1969-1981.

Eberhardt, L.L., 1986. A preliminary appraisal of line transects. *The journal of Wildlife Management* 32, 82-88.

eCognition Developer, 2010. User Guide. Trimble Documentation, Minchin, Germany.

Edwards, T.C., Cutler, D.R., Beard, K.H., Gibson, J., 2007. Predicting invasive plant species occurrences in national parks: a process for prioritizing prevention. Final Project Report No. 2007-1, USGS Utah Cooperative Fish and Wildlife Research Unit, Utah State University, Logan, UT 84322-5290 USA.

Egan, J.P., 1975. Signal detection theory and ROC analysis, Series in Cognition and Perception. Academic Press, New York.

Egberink, J., Pickworth, G., 1969. *Eupatorium odoratum - A* thorny problem. *Farming Journal of South Africa* 45, 25-29.

Emborg, J., 1998. Understorey light conditions and regeneration with respect to the structural dynamics of a near-natural temperate deciduous forest in Denmark. *Forest Ecology and Management* 106, 83-95.

Fawcett, T., 2006. An introduction to ROC analysis. *Pattern Recognition Letters* 27, 861–874.

Felton, A., Felton, A.M., Wood, J., Lindenmayer, D.B., 2006. Vegetation structure, phenology, and regeneration in the natural and anthropogenic tree-fall gaps of a reduced-impact logged subtropical Bolivian forest. *Forest Ecology and Management* 235, 186–193.

Fensham, R.J., Fairfax, R.J., Cannell, R.J., 1994. The invasion of *Lantana camara* (L). in Forty Mile Scrub National Park, north Queensland. *Australian Journal of Ecology* 19, 297–305.

Fielding, A.H., Bell, J.F., 1997. Review methods for the assessment of prediction errors in conservation presence/absence models. *Environmental Conservation* 24, 38-49.

Fourcade, H.G., 1889. Report on the Natal forests, 197 pp. W. Watson, Pietermaritzburg.

Fox, T.J., Knutson, M.G., Hines, R.K., 2000. Mapping forest canopy gaps using air-photo interpretation and ground surveys. *Wildlife Society Bulletin* 28, 882-889.

Fox, J., 2002. Linear mixed models - An R and S-PLUS Companion to Applied Regression.

Franklin J (1995) Predictive vegetation mapping: geographic modeling of biospatial patterns in relation to environmental gradients. *Prog Phys Geog* 19, 474-499.

Gamon, J.A., Field, C.B., Gouldne, M.L., Griffin, K.L., Hartley, A.E., Joel, G., Peñuelas, J., Valentini, R., 1995. Relationship between NDVI, canopy structure and photosynthesis in three Californian vegetation types. *Ecological Applications* 5, 28-41.

Gao, J., 1999. A comparative study on spatial and spectral resolutions of satellite data in mapping mangrove forests. *International Journal of Remote Sensing* 14, 2823-2833.

Gareeb, M., 2007. Investigating in the potted *Chromolaena odorata* (L.) R.M. King and H. Robinson (Asteraceae). Thesis: School of Biological and Conservation Sciences, University of KwaZulu-Natal, Durban South Africa, 3-48.

Geldenhuys, C. J., 1989. Biogeography of the mixed evergreen forests of southern Africa. Ecosystems Programmes Occasional Report no. 45. FRD, Pretoria.

Gentle, C.B., Duggin, J.A., 1998. Interference of *Choricarpia leptopetala* by *Lantana camara* with nutrient enrichment in mesic forests on the Central Coast of NSW. *Plant Ecology* 136, 205- 211.

Gibson, L., Barrett, B., Burbidge, A., 2007. Dealing with uncertain absences in habitat modelling: a case study of a rare ground-dwelling parrot. *Diversity and Distributions* 13, 704–713.

Gitelson, A.A., Merzlyak, M.N., 1994. Spectral Reflectance Changes Associated with Autumn Senescence of Aesculus Hippocastanum L. and Acer Platanoides L. Leaves. Spectral Features and Relation to Chlorophyll Estimation. *Journal of Plant Physiology* 143, 286-292.

Gong, P. Pu, R., Yu, B., 1997. Conifer species recognition: An exploratory analysis of in situ hyperspectral data. *Remote Sensing of Environment* 62, 189-200.

Goodall, J.M., Erasmus, D.J., 1996. Review of the status and integrated control of the invasive weed, *Chromolaena odorata,* in South Africa. *Agriculture, Ecosystem and Environment* 56, 151-164.

Goodall, J.M., Zacharias, P., 2002. Managing *Chromolaena odorata* in subtropical grasslands in KwaZulu-Natal, South Africa. In: Zachariades, C., Muniappan, R., Strathie, L (eds). *Proceedings of the 5th international workshop on biological control and management of Chromolaena odorata*. ARC-PPRI, Pretoria, South Africa, 120-127.

Green, E.P., Clark, C.D., Mumby, P.J., Edwards, A.J., Ellis, A.C., 1998. Remote sensing techniques for mangrove mapping. *International Journal of Remote Sensing* 5,935-956.

Gu, W., Swihart, R.K., 2004. Absent or undetected? Effects of non-detection of species occurrence on wildlife – habitat models. *Biological Conservation* 116, 195-203.

Herren-Gemmill, B. 1991. The ecological role of the exotic asteraceous Chromolaena odorata in the bush fallow farming system of West Africa. *Biotrop. Special Publication* 44, 11-22.

Hestir, E.L., Khanna, S. Andrew, M.E., Santos, M.J., Greenberg, J.A., 2008. Identification of invasive vegetation using hyperspectral remote sensing in the California Delta ecosystems. *Remote Sensing of Environment* 112, 4034-4047.

Hirzel A.H, Guisan, A., 2002.Which is the optimal sampling strategy for habitat suitability modelling? *Ecological Modeling* 157, 331-341.

Hodgson, M. E., Bresnahan, P., 2004. Accuracy of airborne Lidar-derived elevation: empirical assessment and error budget. *Photogrammetric Engineering and Remote Sensing* 70, 331-339.

Holm, L.G., Plucknett, D.L., Pancho, J.V., Herberger, J.P., 1977. The world's worst weeds distribution and biology - University Press of Hawaii, Honolulu.

Horler, D.N.H., Dockray, M., Barber, J., 1983. The red edge of plant leaf reflectance. *International Journal of Remote Sensing* 4, 273–288.

Huete, A.R., H. Liu, K. Batchily, Van Leeuwen, W., 1997. A Comparison of Vegetation Indices over a Global Set of TM Images for EOS-MODIS. *Remote Sensing of Environment* 59, 440-451.

Hutchinson, M. F., 1996. A locally adaptive approach to the interpolation of digital elevation models. In Proceedings, *Third International Conference/Workshop on Integrating GIS and Environmental Modeling*, Santa Fe, NM, January 21-26, 1996. Santa Barbara, CA: National Center for Geographic Information and Analysis.

Immitzer, M., Atzberger, C., Koukal, T., 2012. Tree Species Classification with Random Forest using Very high Spatial Resolution 8-Band WorldView-2 Satellite Data. *Remote Sensing* 4, 2661-2693.

Jackson, R. D., Slater, P. N., Pinter, P. J., 1983: Discrimination of growth and water stress in wheat by various vegetation indices through clear and turbid atmospheres. *Remote Sens. Environ*. 13, 187–208.

Jarošik, V., Pyšek, P., Foxcroft, L.C., Richardson, D.M., Rouget, M., MacFadyen, S., 2011. Predicting Incursion of plant invaders into Kruger National Park, South Africa: The interplay of general drivers and species-specific factors. 6 (12), e28711. *Plos One*. Open Access.

Jiang, Z., Huete, A. R., Didan, K. Miura, T., 2008. Development of a two-band Enhanced Vegetation Index without a blue band. *Remote Sensing of Environment*, 112, 3833-3845.

Joshi, C., de Leeuw, j., Skidmore, A.K., van Andel, J., Lekhak, H.D, van Duren, I.C., 2006. Remote sensing and GIS for mapping and management of invasive shrub *Chromolaena odorata* in Nepal. International Institute for geo-Information Science and Earth Observation (ITC), Enschede, Netherlands.

Kaufman, Y. J., Tanre, D., 1992. Atmospherically resistant vegetation index (ARVI) for EOS-MODIS. *IEEE Transactions on Geoscience and Remote Sensing* 30**,** 261-270.

Kerr, J., Ostrovsky, M., 2003. From space to species: ecological applications for remote sensing. *Trends in Ecology and Evolution* 18, 299-305.

Kim et al., 2009. Individual tree species identification using LiDAR-derived crown structures and intensity data. Doctoral thesis. University of Washington, College of Forest Resources, 1–137.

Knipling, E.B., 1970. Physical and physiological basis for the reflectance of visible and near-infrared radiation from vegetation. *Remote Sensing of Environment* 1, 155-159.

Kolar, C. S., Lodge, D.M., 2001. Progress in invasion biology: predicting invaders. *Trends in Ecology and Evolution*16, 199–204.

Kupfer, J.A., Runkle, J.R., 1996. Early gap successional pathways in a *Fagus-Acer* forest preserve: patterns and determinants. *Journal of Vegetation Science* 7, 247-256.

KZNDAE,2013.http://www.kzndae.gov.za/enus/newsroom/mediaarticles/mediaarticles2012.aspx. Accessed on 10 April 2013.

Laba, M., Smith, S., Richmond, M.E., 2004. Purple loosestrife research and mapping for the Hudson River Valley study area. *Final Report, New York Cooperative Fish and Wildlife Research Unit, Department of Natural Resources, Cornell University, Ithaca, NY.*

Lamb, R., 1988. Ecological and perceptual changes to shrubland associated with *Lantana* invasion. In: Caring for Warringah's Bushland, Shire of Warringah, Sydney.

Le Maitre, D.C., 2002. Invasive alien trees and water resources in South Africa: case studies of the costs and benefits of management. *Forest Ecology and Management* 160, 143–159.

Le Roux, S.D., 2013. Bioclimatic groups of KwaZulu-Natal. Found at http://agriculture.kzntl.gov.za/AgricPublications/ProductionGuidelines/PasturesinKwaZuluNatal/BioclimaticGroupsofNatal/tabid/299/Default.aspx . Accessed on: 18 April 2013.

Lefsky, M.A., Cohen, W.B., Parker, G.G., Harding, D.J., 2000. Lidar remote sensing for ecosystem studies.*BioScience* 52, 19-30.

Lillesand, T.M., Kiefer, R.W., Chipman, J.W., 2004. Remote Sensing and Image Interpretation. Fifth edition. Wiley Press, 418-423.

Luwum, P., 2002. Control of Invasive *Chromolaena odorata*: An evaluation in some land use types in KwaZulu Natal, South Africa.

Macdonald, I., Frame, G., 1988. The invasion of introduced species into nature reserves in tropical savannas and dry woodlands. *Biological Conservation* 44, 67-93.

Mack, R.N., Von Holle, B., Meyerson, L.A., 2007. Assessing invasive alien species across multiple spatial scales: working globally and locally. *Frontiers in Ecology and the Environment* 5, 217–220.

Mallinis, G., Koutsias, N., Tsakiri-Strti, M., Karteris, M., 2008. Object-based classification using Quickbird imagery for delineating forest vegetation polygons in a Mediterranean test site. *ISPRS Journal of Photogrammetry & Remote Sensing* 63, 237-250.

Manel, S, Dias, J.M, Ormerod, S.J.,1999. Comparing discriminant analysis, neural networks and logistic regression for predicting species' distributions: a case study with a Himalayan river bird. *Ecological Modeling* 120, 337– 347.

Margules, C.R., Pressey, R.L., 2000. Systematic Conservation Planning. *Nature* 405, 243-253

Masocha, M, Skidmore, A.K., 2011. Integrating common classifiers with a GIS expert system to increase the accuracy of invasive species mapping. *Int J Appl Earth Observ Geoinfo* 13, 487-494.

Merriam, G., 1988. Landscapes dynamics in farmland. *Trend in Ecological Evolution* 3, 16-20.

Merzlyak, J.R., Gitelson, A.A, Chivkunova, O.B., Rakitin, V.Y., 1999. Non-destructive Optical Detection of Pigment Changes During Leaf Senescence and Fruit Ripening. *Physiologia Plantarum* 106, 135-141.

Moore, A.B., 2004. Alien Invasive species: Impacts on Forests and Forestry. – Forest Health and Biosecurity Working Papers FAO, 66p. Rome, Italy.

Mutanga, O., Adam, E., Cho, M.A., 2012. High density biomass estimation for wetland vegetation using WorldView-2 imagery and random forest regression algorithm. *International Journal of Applied Earth Observation and Geoinformation* 18, 399–406.

Mutanga, O., Skidmore, A.K., 2004. Narrow band vegetation indices solve the saturation problem in biomass estimation. *International Journal of Remote Sensing* 25, 3999-4014.

Naidoo, L., Cho, M.A., Mathieu, R., Asner, G., 2012. Classification of savannah tree species, in the Greater Kruger National Park region, by integrating hyperspectral and LiDAR data in a Random Forest data mining environment. *ISPRS Journal of Photogrammetry and Remote Sensing* 69, 167–179.

Negrón-Juárez, R., I., Chambers, J.Q., Marra, D.M., 2011. Detection of subpixel treefall gaps with Landsat imagery in Central Amazon. *Remote Sensing of Environment* 115, 3322-3328.

Omar, H., 2010. Commercial Timber Tree Species Identification Using Multispectral WorldView-2 Data. Digital Globe® 8 Band Research Challenge.

Oosthuizen, M.J., 1964. The biological control of *Lantana camara* L. in Natal. *Journal of the Entomological Society of Southern Africa* 27, 3-16.

Orians, G. H. ,1982. The influence of tree-falls in tropical forests in tree species richness. *Tropical Ecology* 23: 255–279.

Ozdemir, I., Karnieli, A., 2011. Predicting forest structural parameters using the image texture derived from WorldView-2 multispectral imagery in a dryland forest, Israel. *International Journal of Applied Earth Observation and Geoinformation* 13, 701–710.

Pande, A., Williams, C. L., Lant, C.L., Gibson, D.J., 2006. Using map algebra to determine the mesoscale distribution of invasive plants: the case of *Celastrus orbiculatus* in Southern Illinois, USA. *Biological Invasions.* DOI 10.1007/s10530-006-9049-x.

Peñuelas, J., Baret, F., Filella, I., 1995. Semi-empirical indices to assess carotenoids/chlorophyll a ratio from leaf spectral reflectance. *Photosynthetica* 31**,** 221-230

Peñuelas, J., Filella, L., 1998. Visible and near-infrared reflectance techniques for diagnosing plant physiological status. *Trends in Plant Science* 3, 151-156.

Perumal, K., Bhaskaran, R., 2010. Supervised classification performance of multispectral images. *Journal of Computing* 2, ISSN 2151-9617.

Pu, R., Landry, S., 2012. A comparative analysis of high spatial resolution IKONOS and WorldView-2 imagery for mapping urban tree species. *Remote Sensing of Environment* 124, 516-533.

R Development Core Team., 2005. R: A language and environment for statistical computing, reference index version 2.2.1. R Foundation for Statistical Computing, Vienna, Austria. ISBN 3-900051-07-0, URL http://www.R-project.org.

Ramoelo, A., Skidmore, A.K., Cho, M.A., Schlerf, M., Mathieu, R,, Heitkonig, I.M.A., 2012. Regional estimation of savanna grass nitrogen using the red-edge band of the spaceborne RapidEye sensor, *International Journal of Applied Earth Observation and Geoinformation* 19, 151-162.

Rand, T.A., Russell, F.L., Louda, S.M., 2004. Local- vs. landscape-scale indirect effects of an invasive weed on native plants. *Weed Technology* 18(Suppl S), 1250–1254.

Rew, L.J., Maxwell, B.D., Aspinall, R., 2005. Predicting the occurrence of nonindigenous species using environmental data and remotely sensed data. *Weed Science* 53, 236-241.

Reyers, B., 2004. Incorporating anthropogenic threats into evaluations of regional biodiversity and prioritisation of conservation areas in the Limpopo Province, South Africa. *Biological Conservation* 118, 521–531.

Richards, J.A., Jia, X., 1996. Remote Sensing Digital Image Analysis – An Introduction, Third Edition, Springer.

Rowe, S., 1992. The ecosystem approach to forestland management *Forest Chronicles* 680, 222-224.

Runkle, J.R., 1982. Patterns of disturbance in some old-growth mesic forests of Eastern North-America. *Ecology* 63, 1533–1546

SAS, 2012. The power to know. www.sas.com .

Saura, S., 2001. Influence of scale in landscape architecture: a study using a new method space simulation, satellite images and thematic maps. Ph.D. Thesis, *University of Madrid*.

Scott, J.M., Heglund, P.J., Morrison, M.L., Haufler, J.B., Raphael, M.G., Wall, W.A., Samson, F.B. (Eds.), 2002. Predicting Species Occurrences: Issues of Accuracy and Scale. *Island Press*, Washington, DC.

Sellers, P. J., 1985. Canopy reflectance, photosynthesis, and transpiration. *International Journal of Remote Sensing* 6, 1335-1371.

Sharma, O.P., Makkar, H.P.S., Dawra, R.K., 1988. A review of the noxious plant *Lantana camara*. *Toxicon*. 26, 975–987.

Smith, K.L.,Steven, M.D.,Colls,J.J., 2004. Use of hyperspectral derivative ratios in the rededge region to identify plant stress responses to gas leaks. *Remote Sensing of Environment* 92, 207-217.

Stone, T.A. , Lefebvre, P., 1998. Using multitemporal satellite data to evaluate selective logging in Para, Brazil. *International Journal of Remote Sensing* 19, 2517–2526.

Story, M., Congalton, R., 1986. Accuracy assessment: a user's perspective. *Photogramm. Eng. Remote Sens.* 52, 397-399.

Suarez, A.V., Pfennig, K.S., Robinson, S.K., 1997. Nesting success of a disturbance-dependent sonbird on different kinds of edges. *Conservation Biology* 11, 928-935.

Swets, J.A., Dawes, R.M., Monahan, J., 2000. Better decisions through science. Scientific American 283, 82–87.

Totland, O., Nyeko, P., Bjerknes, A., Hegland, S.J., Nielson, A., 2005. Does forest gap size affect population size, plant size, reproductive success and pollinator visitation in *Lantana camara,* a tropical invasive shrub?. *Forest Ecology and Management* 215, 329–338.

Treitz, P., Lim, K., Wulder, M., Stonge, B. and Flood, M., 2003. LiDAR remote sensing of forest structure. *Progress in Physical Geography* 27,88-106.

Turner, W., Spector, S., Gardiner, N., Fladeland, M., Sterliug, E., 2003. Remote sensing of biodiversity science and conservation. *Trends in Ecology & Evolution* 18, 306-314.

Underwood, E., Ustin, S., DiPietro, D., 2003. Mapping non-native plants using hyperspectral imagery. *Remote Sensing of Environment* 86, 150–161.

Updike, T., Comp, C., 2010. Radiometric Use of WorldView-2 Imagery, DigitalGlobe. Technical Note. DigitalGlobe®, Colorado, USA.

Urgenson, L. S., Reichard, S. H., Halpern, C. B., 2009. Community and ecosystem consequences of giant knotweed (Polygonum sachalinense) invasion into riparian forests of western Washington, USA. *Biological Conservation* 142, 1536–1541.

USGS, 2013. Best Spectral bands to use for vegetation studies with Landsat image. Found at http://landsat.usgs.gov/best_spectral_bands_to_use.php.

Ustin, S. L., Gitelson, A. A., Jacquemoud, S., Schaepman, M., Asner, G. P., Gamon, J. A., et al., 2009. Retrieval of foliar information about plant pigment systems from high resolution spectroscopy. *Remote Sensing of Environment*, 113(Supplement 1), S67–S77.

Ustin, S.L., Trabucco, A., 2000. Using Hyperspectral Data to Assess Forest Structure. *Journal of Forestry* 98, 47-49.

Václavík, T., Meentemeyer, R., 2009. Invasive species distribution modeling (iSDM): Are absence data and dispersal constraints needed to predict actual distributions? *Ecological Modelling* 220, 3248–3258.

Van Der Meer, P.J, Bongers, F., Chatrou, L., Riera, B., 1996. Defining canopy gaps in a tropical rainforest: effects on gap size and turnover time. *Acta Oecologica* 15, 701-714.

Van Gils, H., Mwanangi, M., Rugege, D., 2006. Invasion of an alien shrub across four land management regimes, west of St Lucia, South Africa. *South African Journal of Science* 102, February.

Van Wyk, G.F., Everard, D.A., Modgley, J.J., Gordon, I.G., 1996. Classification and dynamics of a southern African subtropical coastal lowland forest. *South African Journal of Botany* 62, 133-142.

Vepakomma, U., Onge, B.S., Kneeshaw, D., 2008. Spatially explicit characterization of boreal forest gap dynamics using multi-temporal lidar data. *Remote Sensing of Environment* 112, 2326–2340.

Weiss, M. Baret, F., 1999. Evaluation of Canopy Biophysical Variable Retrieval Performances from the Accumulation of Large Swath Satellite Data. *Remote Sensing of Environment* 70, 293-306.

Weiss, P.W., Noble, I.R., 1984. Status of coastal dune communities invaded by *Chrysanthemoides monilifera*. *Australian Journal of Ecology* 9, 93–98.

Whitmore, T.C., 1989. Canopy gaps and the two major groups of forest trees. Special feature – Treefall gaps and forest dynamics. *Ecology* 70, 536–538.

Wolter, P.T., Townsend, P.A., Sturtevant, B.R., 2009. Estimation of forest structural parameters using 5 and 10 meter SPOT-5 satellite data. *Remote Sensing of Environment* 113, 2019–2036.

Woodcock, C. E., Macomber, S. A., Pax-Lenney, M., Cohen, W. C., 2001. Monitoring large areas for forest change using Landsat: Generalization across space, time and Landsat sensors. *Remote Sensing of Environment* 78, 194–203.

Wulder, M.A., Deshka, J.A., Gillis, M.A., Luther, J.E., Hall, R.J., Beaudouin, A., Franklin, S.E., 2003. Operational mapping of the land cover of the forested area of Canada with Landsat data: EOSD land cover program. *Forest Chronicles* 79, 1075–1083.

Yamamoto, S., 1992. The Gap Theory in Forest Dynamics. *Botanical Magazine*. Tokyo. 105: 375-383.

Yan, G., Mas, J.F., Maathuis, B.H.P., Xiangmin, Z., Van Dijk, P.M., 2007. Comparison of pixel-based and object-oriented image classification approaches—a case study in a coal fire area, Wuda, Inner Mongolia, China. *International Journal of Remote Sensing* 27, 4039-4055.

Yan, X., Su, X., 2009. Linear Regression Analysis: Theory and Computing. World Scientific Publishing Co. Pte. Ltd.

Yang, X., Skidmore, A.K., Melick, D.R., Shou, Z., Xu, J., 2006. Mapping non-wood forest product (matsutake mushrooms) using logistic regression and GIS expert system. *Ecological Modelling* 198, 208–218.

Zedler, P. H., Scheid, G. A., 1988. Invasion of *Carpobrotus edulis* and *Salix lasiolepis* after fire in a coastal chaparral site in Santa Barbara County, California. *Madrono* 35, 196–201.

Zhou, Q., Robson, M., 2001. Automated rangeland vegetation cover and density estimation using ground digital images and a spectral-contextual classifier. *International Journal of Remote Sensing* 22, 3457 – 3470.

Zhou, Z., Jancso, T., Chen, C., Verone, M., 2012. Urban Land Cover Mapping Based on Object Oreinted Classification Using WorldView-2 Satellite Remote Sensing Images. *International Scientific Conference on Sustainable Development and Ecological Footprint*, Sopron, Hungary.

APPENDICES

Appendix A

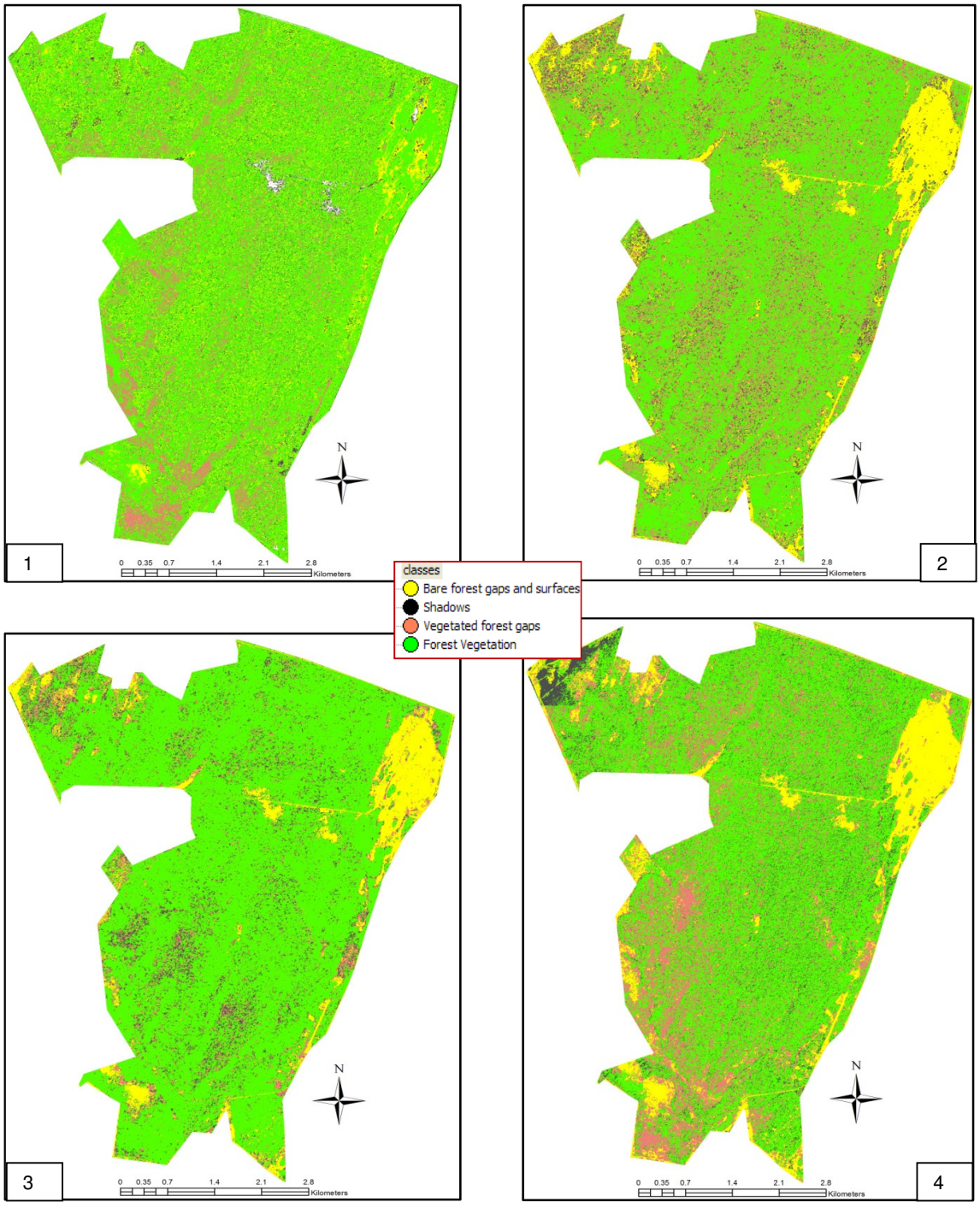

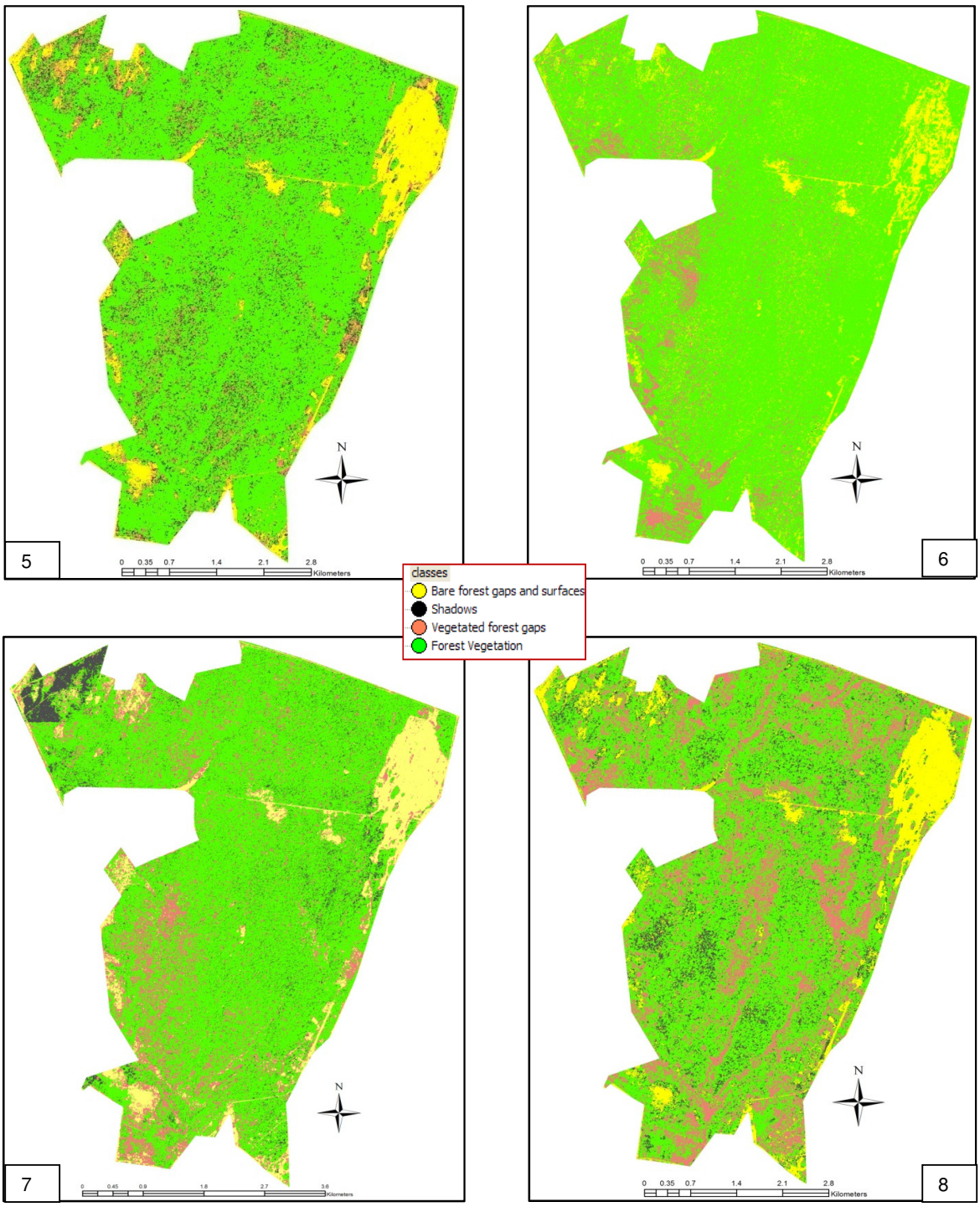
5
6
7
8
N
0 0.35 0.7 1.4 2.1 2.8
Kilometers
0 0.45 0.9 1.8 2.7 3.6
classes
Bare forest gaps and surfaces
Shadows
Vegetated forest gaps
Forest Vegetation

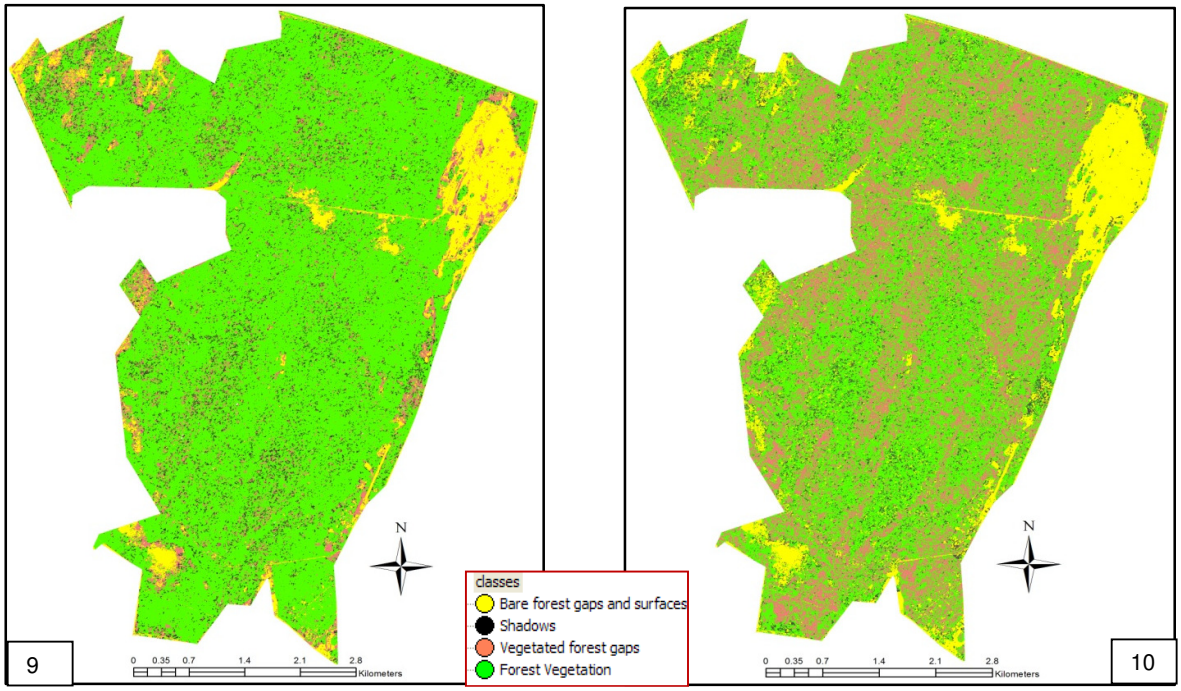

Figs. A Results of object-based classification based on 10 vegetation indices derived from WordView-2 image data. Indices are arranged alphabetically as follows: 1 = ARVI, 2 = EVI, 3 = $NDVI_{545}$, 4 = mPSRI, 5 = $NDVI_{RED}$, 6 = $NDVI_{NIR}$, 7 = NPCI, 8 = $NDVI_{725}$, 9 = YI, 10 = $NDVI_{605}$.

Appendix B

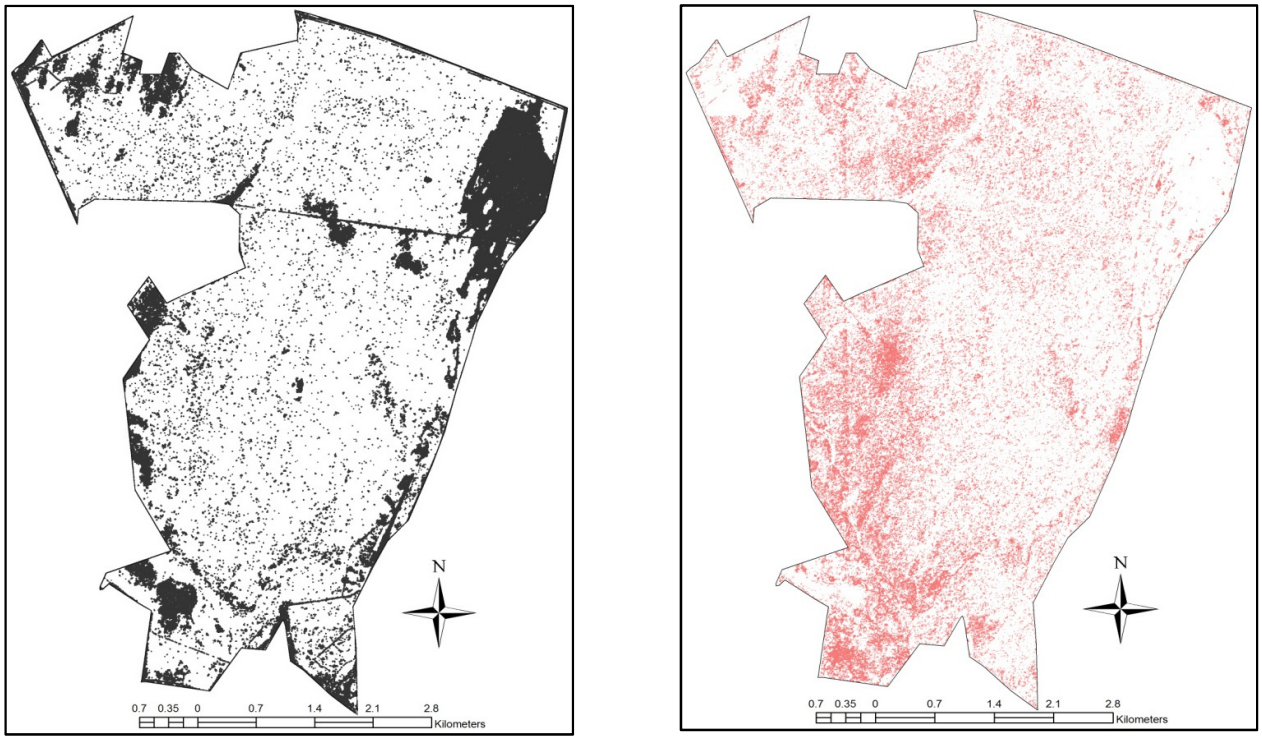

Figs. B A side-by-side presentation of bare forest gaps and surfaces (a) and vegetated forest gaps (b) derived from mPSRI in object-based classification. The mPSR index shows high overall accuracy over all

Appendix C

Error matrices of different classification methods (Bare = bare forest gaps and surfaces, Vegetated = vegetated gaps, Shadow = shadow gaps, Other = other forest vegetation)

(a) Minimum Distance Classifier

		Reference Image					
	Class	Bar_gaps	Vegetated	Shadow	Other	Total	*User Accuracy*
Classified Image	Bare	**21**	2	0	0	27	96.00
	Vegetated	5	**17**	2	13	19	89.47
	Shadow	7	0	**12**	0	19	63.16
	Other	3	4	3	**23**	46	50.00
	Total	36	23	24	28	111	
	Producer Accuracy%	58.33	73.91	50.00	82.14		
	Kappa Index					0.52	
	Overall Accuracy					68.46	

(b) Parallelepiped Classifier

		Reference Image					
	Class	Bare	Vegetated	Shadow	Other	Total	*User Accuracy*
Classified Image	Bare	**21**	3	2	3	27	77.77
	Vegetated	2	**9**	4	4	19	47.37
	Shadow	0	5	**11**	2	19	57.90
	Other	2	5	7	**32**	46	69.57
	Total	25	22	24	41	111	
	Producer Accuracy%	84.00	40.91	45.83	78.05		
	Kappa Index					0.49	
	Overall Accuracy					65.76	

(c) Maximum likelihood classifier (8 bands)

	Reference Image					
Classified Image	Class	Bare	Vegetated	Shadow	Other	Total	*User Accuracy*
	Bare	**23**	2	1	1	27	85.19
	Vegetated	1	**16**	0	2	19	84.21
	Shadow	0	0	**18**	1	19	94.74
	Other	1	3	3	**39**	46	80.43
	Total	25	21	22	43	111	
	Producer Accuracy%	92.00	76.19	81.82	90.70		
	Kappa Index					0.82	
	Overall Accuracy					86.90	

(d) Object-based classification using NPCI

	Reference Image					
Classified Image	Class	Bare	Vegetated	Shadow	Other	Total	*User Accuracy*
	Bare	**27**	0	0	0	27	100
	Vegetated	0	**10**	9	0	19	52.63
	Shadow	1	6	**11**	1	19	57.90
	Other	2	3	1	**40**	46	86.96
	Total	30	19	21	41	111	
	Producer Accuracy%	90.00	52.63	52.38	97.56		
	Kappa Index					0.70	
	Overall Accuracy					79.28	

1 Object-based classification using ARVI

		Reference Image					
Classified Image	Class	Bare	Vegetated	Shadow	Other	Total	*User Accuracy*
	Bare	**9**	0	14	4	27	33.33
	Vegetated	2	**9**	3	5	19	47.37
	Shadow	6	0	**12**	1	19	63.16
	Other	1	0	0	**45**	46	97.83
	Total	18	9	29	55	111	
	Producer Accuracy%	50.00	100.00	41.38	81.81		
	Kappa Index					0.68	
	Overall Accuracy					67.57	

2 Object-based classification using EVI

		Reference Image					
Classified Image	Class	Bare	Vegetated	Shadow	Other	Total	*User Accuracy*
	Bare	**27**	0	0	0	27	100.00
	Vegetated	4	**11**	1	3	19	57.89
	Shadow	2	3	**12**	2	19	63.16
	Other	1	4	1	**40**	46	86.96
	Total	34	18	14	45	111	
	Producer Accuracy%	79.41	61.11	85.71	88.89		
	Kappa Index					0.79	
	Overall Accuracy					81.08	

3 Object-based classification using $NDVI_{545}$

	Reference Image					
Classified Image	Class	Bare	Vegetated	Shadow	Other	Total	*User Accuracy*
	Bare	**27**	0	0	0	27	100.00
	Vegetated	3	**12**	1	3	19	63.16
	Shadow	1	1	**13**	4	19	68.42
	Other	1	4	1	**40**	46	86.96
	Total	32	17	15	47	111	
	Producer Accuracy%	84.38	70.59	86.67	85.11		
	Kappa Index					0.78	
	Overall Accuracy					82.88	

4 Object-based classification using mPSRI

	Reference Image					
Classified Image	Class	Bare	Vegetated	Shadow	Other	Total	*User Accuracy*
	Bare	**26**	0	1	0	27	96.30
	Vegetated	1	**16**	1	1	19	84.21
	Shadow	0	0	**19**	0	19	100.00
	Other	0	2	1	**43**	46	93.48
	Total	27	19	21	44	111	
	Producer Accuracy%	96.29	84.21	90.48	97.73		
	Kappa Index					0.91	
	Overall Accuracy					93.69	

5 Object-based classification using $NDVI_{660}$

		Reference Image					
	Class	Bare	Vegetated	Shadow	Other	Total	*User Accuracy*
Classified Image	Bare	**27**	0	0	0	27	100.00
	Vegetated	0	**10**	2	7	19	52.63
	Shadow	2	1	**9**	8	19	47.37
	Other	0	1	0	**45**	46	97.83
	Total	29	12	11	60	111	
	Producer Accuracy%	93.10	83.33	81.82	75.00		
	Kappa Index					0.73	
	Overall Accuracy					78.38	

6 Object-based classification using $NDVI_{NIR}$

		Reference Image					
	Class	Bare	Vegetated	Shadow	Other	Total	*User Accuracy*
Classified Image	Bare	**25**	0	0	2	27	92.59
	Vegetated	2	**9**	2	6	19	47.37
	Shadow	4	3	**7**	5	19	36.84
	Other	1	3	16	**26**	46	56.52
	Total	32	15	25	39	111	
	Producer Accuracy%	78.13	60.00	28.00	66.67		
	Kappa Index					0.63	
	Overall Accuracy					60.36	

7 Object-based classification using NPCI

		Reference Image					
	Class	Bare	Vegetated	Shadow	Other	Total	*User Accuracy*
Classified Image	Bare	**27**	0	0	0	27	100
	Vegetated	0	**10**	9	0	19	52.63
	Shadow	1	6	**11**	1	19	57.90
	Other	2	3	1	**40**	46	86.96
	Total	30	19	21	41	111	
	Producer Accuracy%	90.00	52.63	52.38	97.56		
	Kappa Index					0.70	
	Overall Accuracy					79.28	

8 Object-based classification using $NDVI_{725}$

		Reference Image					
	Class	Bare	Vegetated	Shadow	Other	Total	*User Accuracy*
Classified Image	Bare	**26**	0	0	1	27	96.30
	Vegetated	1	**17**	0	1	19	89.47
	Shadow	6	0	**10**	3	19	52.63
	Other	3	4	0	**39**	46	84.78
	Total	35	21	10	44	111	
	Producer Accuracy%	74.29	80.95	100	88.64		
	Kappa Index					0.76	
	Overall Accuracy					82.88	

9 Object-based classification using YI

		Reference Image					
Classified Image	Class	Bare	Vegetated	Shadow	Other	Total	*User Accuracy*
	Bare	**24**	2	0	1	27	88.89
	Vegetated	1	**10**	2	6	19	52.63
	Shadow	4	3	**07**	2	19	36.84
	Other	1	3	16	**26**	46	56.52
	Total	30	18	25	35	111	
	Producer Accuracy%	80.00	55.56	28.0	74.29		
	Kappa Index					0.45	
	Overall Accuracy					60.36	

10 Object-based classification using $NDVI_{605}$

		Reference Image					
Classified Image	Class	Bare	Vegetated	Shadow	Other	Total	*User Accuracy*
	Bare	**27**	0	0	0	27	100.00
	Vegetated	4	**12**	3	0	19	63.16
	Shadow	3	3	**8**	5	19	42.11
	Other	7	2	5	**32**	46	69.57
	Total	41	17	16	37	111	
	Producer Accuracy%	65.85	70.59	50.00	86.49		
	Kappa Index					0.71	
	Overall Accuracy					71.17	

11 Maximum likelihood classification results on 4 common visible-near infrared bands

	Reference Image					
Classified Image	Class	Bare	Vegetated	Shadow	Other	Total	*User Accuracy*
	Bare	**19**	1	3	4	27	70.37
	Vegetated	0	**11**	3	5	19	57.89
	Shadow	1	0	**14**	4	19	73.68
	Other	3	3	6	**34**	47	72.34
	Total	23	15	26	47	111	
	Producer Accuracy%	82.60	73.33	53.85	72.34		
	Kappa Index					0.63	
	Overall Accuracy					74.64	